

NUCLEAR DATA AND MEASUREMENTS SERIES

ANL/NDM-47

Scattering of MeV Neutrons from Elemental Iron

by

A. Smith and P. Guenther

March 1979

**ARGONNE NATIONAL LABORATORY,
ARGONNE, ILLINOIS 60439, U.S.A.**

NUCLEAR DATA AND MEASUREMENTS SERIES

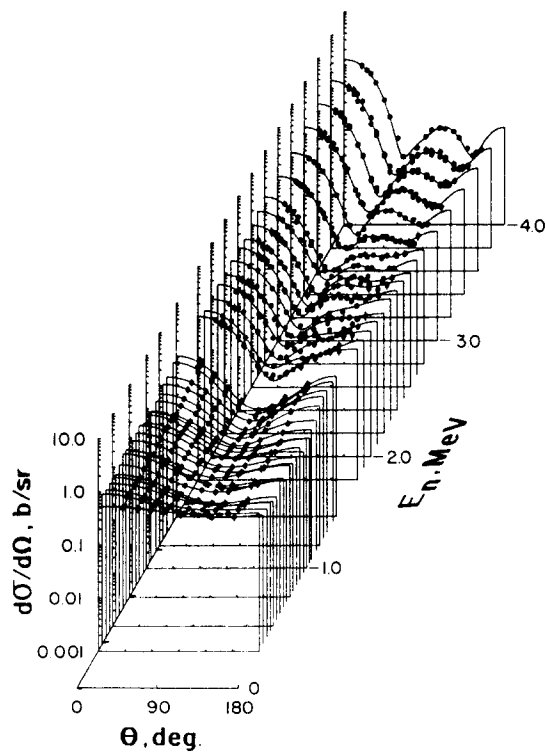
ANL/NDM-47

SCATTERING OF MeV NEUTRONS FROM ELEMENTAL IRON

by

A. Smith and P. Guenther

March 1979



U of C. AUA. USERDA

ARGONNE NATIONAL LABORATORY,
ARGONNE, ILLINOIS 60439, U.S.A.

The facilities of Argonne National Laboratory are owned by the United States Government. Under the terms of a contract (W-31-109-Eng-38) between the U. S. Atomic Energy Commission, Argonne Universities Association and The University of Chicago, the University employs the staff and operates the Laboratory in accordance with policies and programs formulated, approved and reviewed by the Association.

MEMBERS OF ARGONNE UNIVERSITIES ASSOCIATION

The University of Arizona
Carnegie-Mellon University
Case Western Reserve University
The University of Chicago
University of Cincinnati
Illinois Institute of Technology
University of Illinois
Indiana University
Iowa State University
The University of Iowa

Kansas State University
The University of Kansas
Loyola University
Marquette University
Michigan State University
The University of Michigan
University of Minnesota
University of Missouri
Northwestern University
University of Notre Dame

The Ohio State University
Ohio University
The Pennsylvania State University
Purdue University
Saint Louis University
Southern Illinois University
The University of Texas at Austin
Washington University
Wayne State University
The University of Wisconsin

NOTICE

This report was prepared as an account of work sponsored by the United States Government. Neither the United States nor the United States Atomic Energy Commission, nor any of their employees, nor any of their contractors, subcontractors, or their employees, makes any warranty, express or implied, or assumes any legal liability or responsibility for the accuracy, completeness or usefulness of any information, apparatus, product or process disclosed, or represents that its use would not infringe privately-owned rights.

ANL/NDM-47

SCATTERING OF MeV NEUTRONS FROM ELEMENTAL IRON

by

A. Smith and P. Guenther

March 1979

In October 1977, the U.S. Energy Research and Development Agency (ERDA) was incorporated into the U.S. Department of Energy. The research and development functions of the former U.S. Atomic Energy Commission had previously been incorporated into ERDA in January 1975.

Applied Physics Division
Argonne National Laboratory
9700 South Cass Avenue
Argonne, Illinois 60439
USA

NUCLEAR DATA AND MEASUREMENTS SERIES

The Nuclear Data and Measurements Series presents results of studies in the field of microscopic nuclear data. The primary objective is the dissemination of information in the comprehensive form required for nuclear technology applications. This Series is devoted to: a) measured microscopic nuclear parameters, b) experimental techniques and facilities employed in measurements, c) the analysis, correlation and interpretation of nuclear data, and d) the evaluation of nuclear data. Contributions to this Series are reviewed to assure technical competence and, unless otherwise stated, the contents can be formally referenced. This Series does not supplant formal journal publication but it does provide the more extensive information required for technological applications (e.g., tabulated numerical data) in a timely manner.

TABLE OF CONTENTS

	<u>Page</u>
ABSTRACT.	1
I. INTRODUCTION.	2
II. EXPERIMENTAL METHODS.	2
III. EXPERIMENTAL RESULTS.	3
IV. INTERPRETATION.	14
V. EVALUATED SCATTERING CROSS SECTIONS	22
VI. SUMMARY REMARK.	25
APPENDIX.	28
ACKNOWLEDGEMENTS.	35
REFERENCES.	36

SCATTERING OF MeV NEUTRONS FROM ELEMENTAL IRON*

by

A. Smith and P. Guenther

Argonne National Laboratory
Argonne, Illinois

ABSTRACT

Neutron elastic- and inelastic-scattering cross sections of elemental iron are measured from 1.5 to 4.0 MeV with incident-neutron resolutions of ~ 50 keV and at incident-neutron energy intervals of ~ 50 keV. Cross sections for the excitation of observed levels at 0.853, 1.389, 2.097, 2.579, 2.677, 2.974 and 3.152 MeV are determined. The observed elastic- and inelastic-scattering angular distributions fluctuate strongly with incident energy. The experimental results are averaged over broad energy intervals and interpreted in terms of spherical optical-statistical and coupled-channels models including consideration of direct-vibrational excitations. The importance of a comprehensive data base in such energy-averaged interpretations and of the direct-vibrational excitations is stressed. The present measured and calculated results, combined with those reported in the literature, are used to formulate an evaluated scattered-neutron data file in the ENDF format extending from 1.0 to 4.0 MeV.

*This work supported by the U.S. Department of Energy.

I. INTRODUCTION

The scattering of few MeV neutrons from elemental iron ($\sim 92\%$ ^{56}Fe and $\sim 6\%$ ^{54}Fe) is governed by direct- and compound-nucleus processes including the excitation of one and two phonon vibrational levels. The physical interpretation of the observed phenomena is complicated by pronounced fluctuating structure in both elastic- and inelastic-scattering channels. The available experimental data generally is of insufficient scope to reasonably define an energy-averaged behavior consistent with the underlying postulates of the optical-statistical (OS) or coupled-channels (CC) models. It was an objective of the present work to provide a sufficiently detailed experimental data base to reliably define the energy-averaged behavior of neutron scattering from elemental iron and to use this energy-averaged behavior to examine the interplay between compound-nucleus and direct-reaction neutron scattering mechanisms particularly including the excitation of low-lying vibrational levels. Another objective was the provision of experimental-neutron-scattering data for applied needs (e.g. fission-reactor systems) over an energy region extending from that of detailed resonance formulations (e.g. ~ 1.0 MeV) to that of the statistical continuum (e.g. ~ 5 MeV). Section II of this paper briefly outlines the experimental method. The experimental results are described in Sec. III and discussed in terms of spherical (OS) and vibrational (CC) models in Sec. IV. Section V outlines an evaluated scattered-neutron data file for iron over the region 1.0 to 4.0 MeV, derived from the present measured and calculated results and those previously reported in the literature.

II. EXPERIMENTAL METHODS

All of the present measurements employed the pulsed-beam fast-neutron time-of-flight technique and the associated apparatus at the Argonne Fast Neutron Generator. The details of the particular applications of the method and the apparatus have been extensively described elsewhere.^{1,2,3} Therefore, the present remarks are limited to a brief outline of the experimental method.

The ${}^7\text{Li}(p,n){}^7\text{Be}$ reaction was used as a neutron source for all of the measurements.⁴ The lithium-target thicknesses were adjusted to provide incident-neutron energy spreads at the scattering samples of ~ 35 to 40 keV. The energy scale was determined by control of the proton beam and conservatively known to 10 keV; i.e. to a value less than the incident-neutron energy spread. The source was pulsed for durations of ~ 1 nsec at a repetition rate of 2 Mhz.

The scattering samples were right cylinders of high-purity natural iron 2 cm in diameter and 2 cm long. The atomic density was obtained using conventional weight and dimensional measurement techniques. The samples were placed ~ 13 cm from the source at a zero-degree source-reaction angle. The neutrons were incident upon the lateral surface of the cylinders. Similar samples of polyethylene (CH_2) and natural carbon were used for calibration and verification purposes.

Measurements were concurrently made with ten proton-recoil scintillation detectors placed at flight paths of 5 to 5.5 m measured from the scattering sample. The flight paths were defined by a massive-collimator system and distributed over a scattered-neutron angular range of 20 to 160 deg. The velocity resolution of the detection system was sufficient to resolve all prominent scattered-neutron groups resulting from reported levels to excitations of ~ 3.0 MeV. The relative scattering angles were optically determined to within $\pm \sim 0.5$ deg. and the absolute normalization of the relative angular system was determined to be ± 1 deg. by observation of the energy loss of neutrons scattered from hydrogen both left and right of the zero reaction angle. Angular distributions were determined with either a single setting of the collimator system (10 angles) or redundant settings (20 or more angles).

The relative energy dependences of the detector sensitivities were determined either by observation of neutrons emitted at the spontaneous fission of ^{252}Cf or of neutrons scattered from hydrogen at a number of angles with a fixed incident-neutron energy. Generally, results obtained with the two methods were consistent. The relative detector responses were normalized to the wellknown $\text{H}(n;n)$ cross sections by the observation of neutrons scattered from hydrogen at selected incident energies and scattering angles.⁵ Thus all the iron neutron scattering cross sections were determined relative to the $\text{H}(n;n)$ cross sections.

Data acquisition was carried out using a digital computer system which concurrently recorded 512 time intervals and 16 energy-response intervals for each of 11 time-of-flight detectors (10 scattered-neutron and 1 monitor detector). Subsequent data reduction procedures included corrections for angular resolution, sample attenuation and multiple-event effects.³

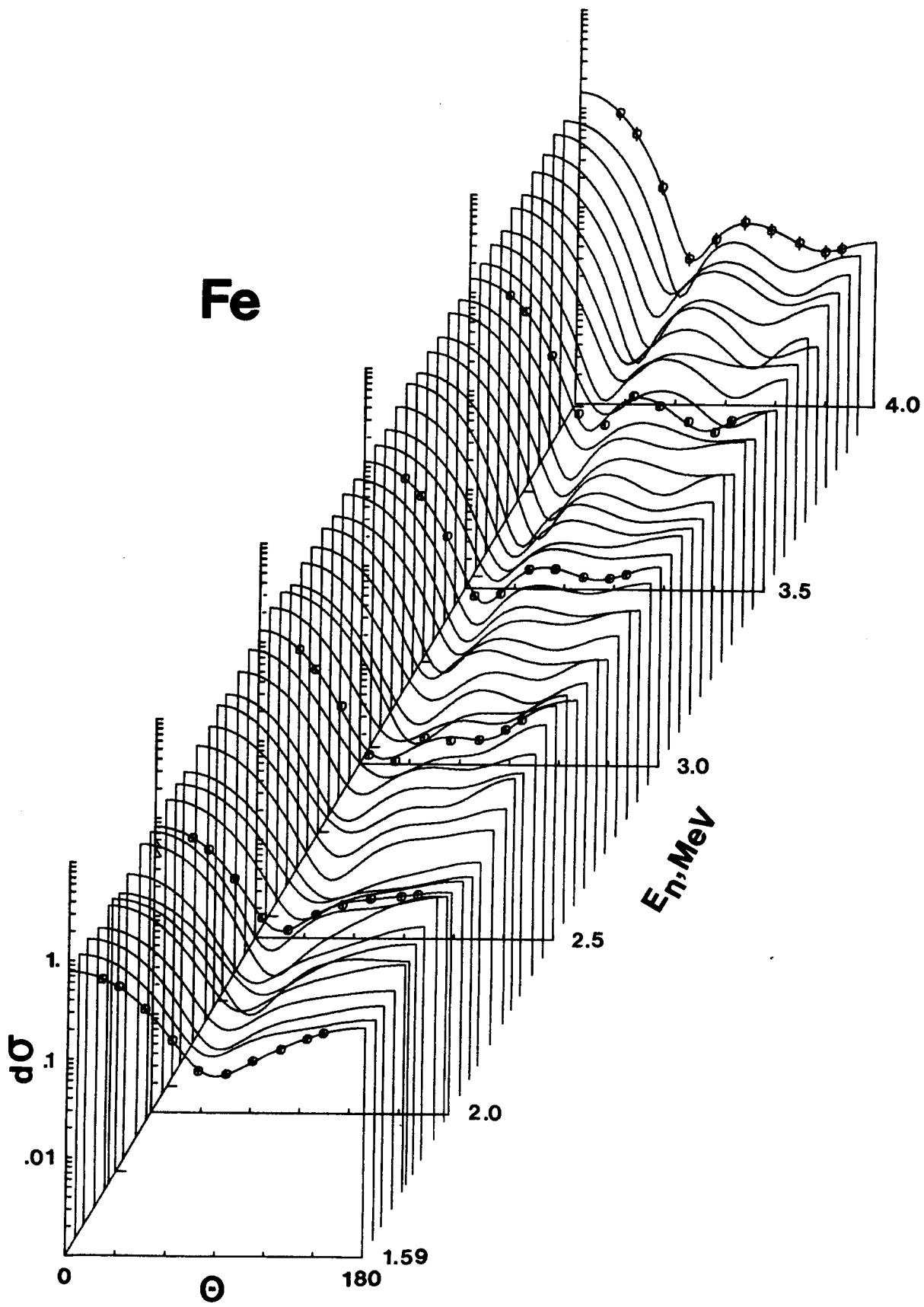
Measurements were made at various periods over a ~ 5 year interval with independent detector calibrations and with detailed variations of the measurement system. The measurement schedules included both random and systematic selection of incident-neutron energies.

III. EXPERIMENTAL RESULTS

A. Neutron Elastic Scattering

A characteristic of the observed differential neutron elastic scattering was a strong fluctuation with incident neutron energy. Even results obtained at the same incident neutron energy varied due to differences in incident resolutions and small variations in energy scale. Thus comparisons of the measured distributions or with the predictions of theory were meaningful only in a relatively broad energy-average. The magnitude of the fluctuations is illustrated by the present neutron-elastic-scattering results shown in Fig. 1. Even with the relatively broad experimental resolutions employed in the present experiments, differential cross sections at some angles can vary by a factor of as much as two in 50 to 100 keV.

Fig. 1. Measured Differential-Elastic-Scattering Cross Sections of Elemental Iron. The present results are illustrated by data points and curves derived by fitting a legendre polynomial series to the measured values. Large fluctuations are evident. Cross section is given in b/sr and scattering angle in lab-deg.



In view of the above fluctuations and the objective of determining energy-averaged behavior, the differential elastic-scattering distributions were averaged over incident-neutron energy intervals of ~ 200 keV. Each averaging interval contained at least five measured distributions. The resulting energy-averaged distributions behaved in a relatively energy-smooth manner as illustrated in Fig. 2. The experimental uncertainties in these energy-averaged differential cross-section values were 3-5%. Of this, $\sim 1\%$ was due to counting statistics. Uncertainty contributions due to the standard-reference H(n;n) cross sections were small ($\sim 1\%$). Corrections for multiple events, angular resolution and beam attenuation effects contributed $\sim 3\%$ to the overall uncertainty. These correction-associated uncertainties could be systematic as detailed resonance-structure effects could not be treated in the correction procedures. Uncertainties due to detector normalizations were generally 3%.

The energy-averaged angle-integrated neutron elastic scattering cross sections were deduced by least-square fitting the corresponding differential distributions with the Legendre polynomial expansion

$$\frac{d\sigma}{d\Omega} = \frac{\sigma}{4\pi} \left[1 + \sum_{i=1}^6 W_i P_i \right]. \quad (1)$$

There were no constraints on the fitting procedure. The resulting angle-integrated elastic-scattering-cross-section values are shown in Fig. 3. Their uncertainties were estimated to be 3-5%. The angle-integrated cross section values generally follow a relatively smooth energy dependence but a broad structure persists even in this 200 keV average. The angle-integrated elastic-scattering cross sections, together with the total cross section, imply a non-elastic cross section. Harvey et al.⁶ have reported high resolution neutron total cross sections over a wide energy range. Smith and Whalen⁷ have shown that an energy-average of the results of Ref. 6 are consistent with the results of broad resolution total cross section measurements to within $\sim 1\%$. Thus a 200 keV average of the results of Harvey et al. was accepted for the derivation of the non-elastic cross sections. The average of the total cross-section results of Ref. 6 and the present energy-averaged elastic-scattering results were subtracted to obtain the non-elastic cross sections shown in Fig. 3. The derivation was extended below 1.5 MeV using an average of previously reported results from this Laboratory.⁸ Fluctuations in the non-elastic cross section are, in part, artifacts of the procedures used to construct average total and elastic-scattering cross sections but the general trend of the non-elastic cross section is defined to within 5-10%. Over the energy range of the present work the non-elastic cross section is comparable with the neutron inelastic-scattering cross section. A 200 keV average of the neutron inelastic-scattering cross sections given in ENDF/B-IV⁹ is compared with the deduced non-elastic cross section in Fig. 3. The averaged ENDF/B-IV inelastic cross section is in good agreement with the present non-elastic result up to energies of ~ 2.0 MeV. Above ~ 2.0 MeV the present non-elastic

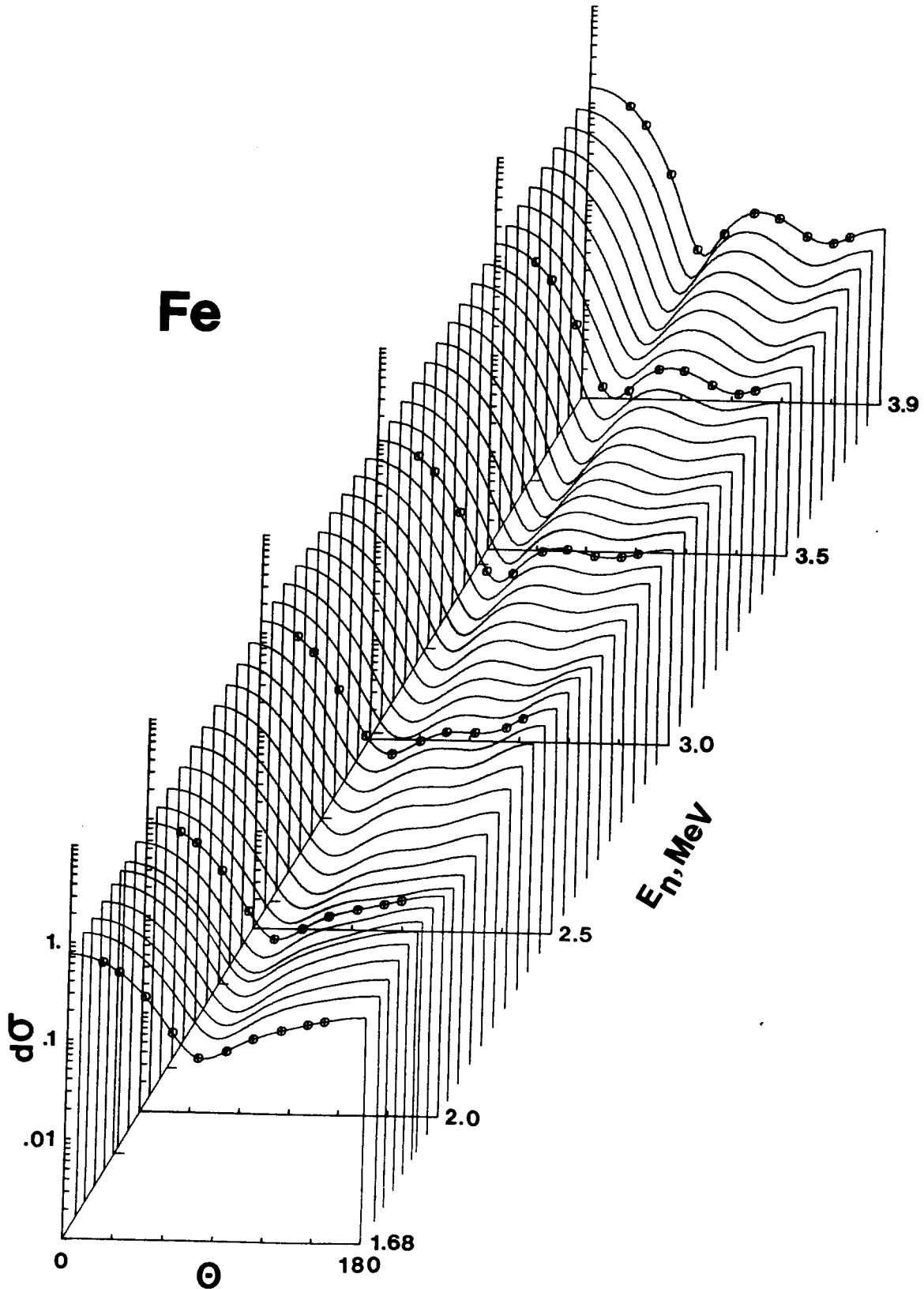
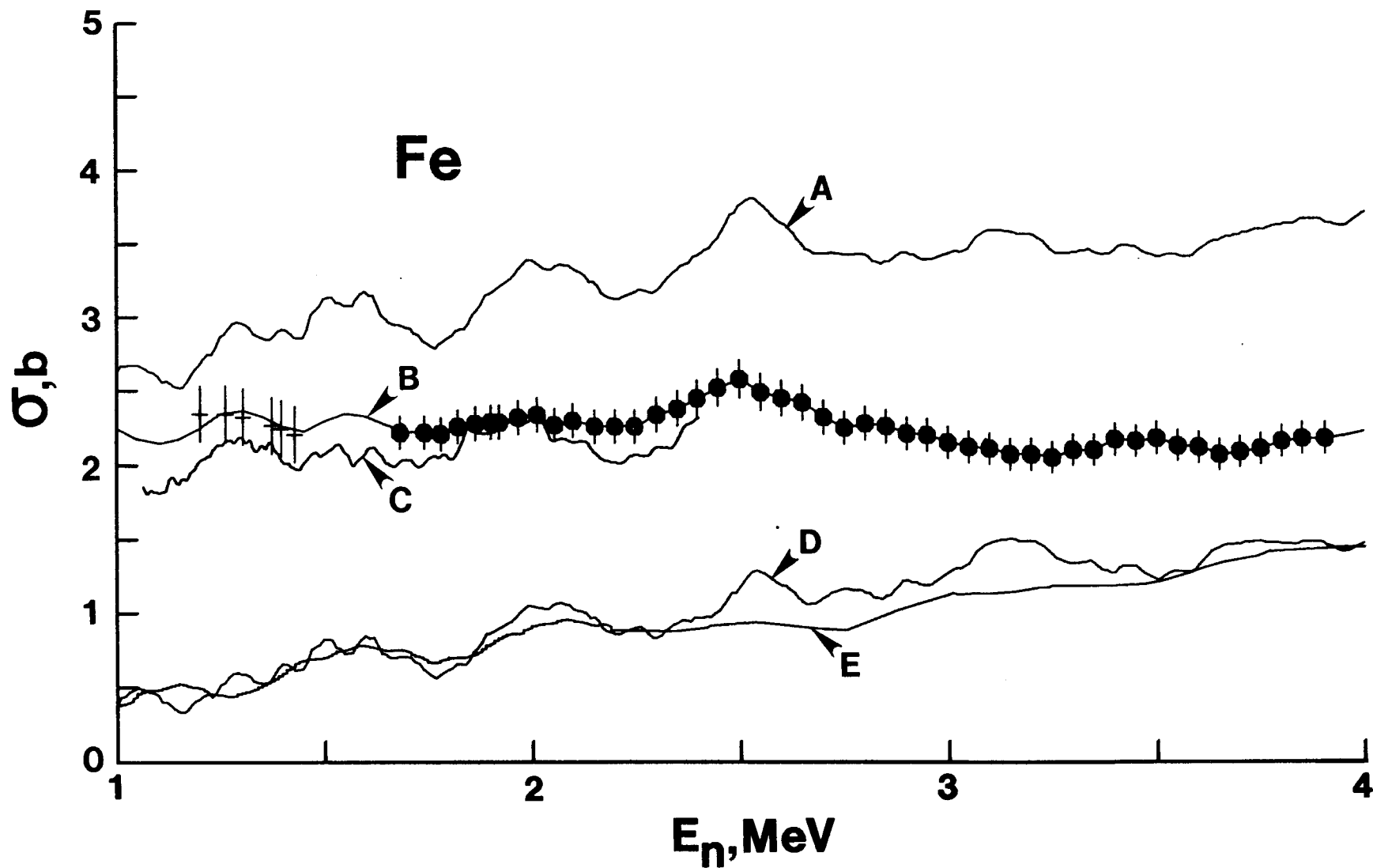


Fig. 2. The Present Measured Differential-Elastic-Scattering Cross Sections of Elemental Iron Averaged Over Incident-Energy Intervals of 200 keV. The notation is identical to that of Fig. 1.

Fig. 3. Comparison of Neutron Cross Sections of Elemental Iron Averaged Over Energy Intervals of 200 keV. The present angle-integrated elastic scattering results are indicated by solid data points, those of Ref. 8 by crosses. The curves denote; A = an equivalent 200 keV average of the total-cross-section results of Ref. 6, B = "eye-guide" constructed through the present experimental values, C = an equivalent average of the elastic-scattering results of Ref. 21, D = the non-elastic cross section as defined in the text, and E = the equivalent average of the neutron inelastic-scattering cross sections as given in ENDF/B-IV.⁹



results are systematically larger than the averaged ENDF/B-IV inelastic values by amounts generally in the range 10-20% (i.e. by factors of 2-4 times the uncertainty in the non-elastic cross section). These non-elastic and inelastic comparisons imply an increase in the iron inelastic scattering cross section above 2.0 MeV, relative to the values of ENDF/B-IV, by appreciable amounts. Such an increase is further supported by the measurements of individual-inelastic-excitation functions as discussed below.

A number of previous measurements of neutron elastic scattering from iron have been reported in the literature (e.g. see Refs. 10-20). These previous results generally pertain to energy-isolated measurements made with various energy resolutions and scales. As a consequence, data comparisons are sensitive to fluctuating structure and agreement (or lack thereof) between various measured results is of uncertain significance. The large variations observed in such isolated comparisons are illustrated in Fig. 4. Perey et al.²¹ have measured elastic scattering from iron with very good resolution up to energies of ~ 2.5 MeV. 200 keV averages of their results were compared with the present measurements. The averaged differential distributions are in qualitative agreement but there are quantitative and systematic differences at some scattering angles (notably between 90-120 deg.). Associated quantitative discrepancies appear in comparisons of angle-integrated cross section values, as illustrated in Fig. 3, with the average values of Ref. 21 tending to be 5-10% lower in magnitude than those derived from the present work. Thus the results of Ref. 21 imply even larger inelastic scattering cross sections than do the results of the present work.

B. Neutron Inelastic Scattering

Neutron groups corresponding to the seven excitation energies 853 ± 15 , 1389 ± 30 , 2097 ± 22 , 2579 ± 35 , 2677 ± 14 , 2974 ± 11 and 3152 ± 21 keV were observed. These excitation energies were determined from the measured scattered-neutron flight times, flight paths and incident-neutron energies. The individual results were averaged to obtain the above mean values with the uncertainties defined as the RMS deviation from the mean of the individual measured values. The observed excitations were generally consistent with reported structure in ^{54}Fe and ^{56}Fe as shown in Table 1.²² The measured differential neutron-inelastic-scattering cross sections fluctuated with incident energy in a manner similar to that of the elastic-scattering cross sections discussed above. Therefore the measured values were averaged over energy increments to obtain the energy-averaged behavior. The averaging increments ranged from 200 keV where the data spanned wide energy ranges (e.g. for the 853 keV state) to 100 keV where the data were of limited energy extent (e.g. for the 3152 keV state). The averaged differential inelastic-scattering cross sections were generally symmetric about 90 deg. excepting those pertaining to the excitation of the 853 keV state. Angle-integrated inelastic scattering cross sections were derived from the averaged differential values using the Legendre fitting procedure described above in the context of elastic scattering. The estimated uncertainties associated with the measured differential inelastic cross sections varied from 5 to 25% depending upon the particular incident energy and excited state. The uncertainties associated with the angle-integrated values were

Fig. 4. Comparison of Measured Differential Elastic Scattering Cross Sections. Present results are indicated by solid data points and curves. Previously reported results are indicated by various symbols as defined in the reference list. Energies are numerically noted in the MeV. Cross sections are given in b/sr and scattering angle (θ) in lab deg.

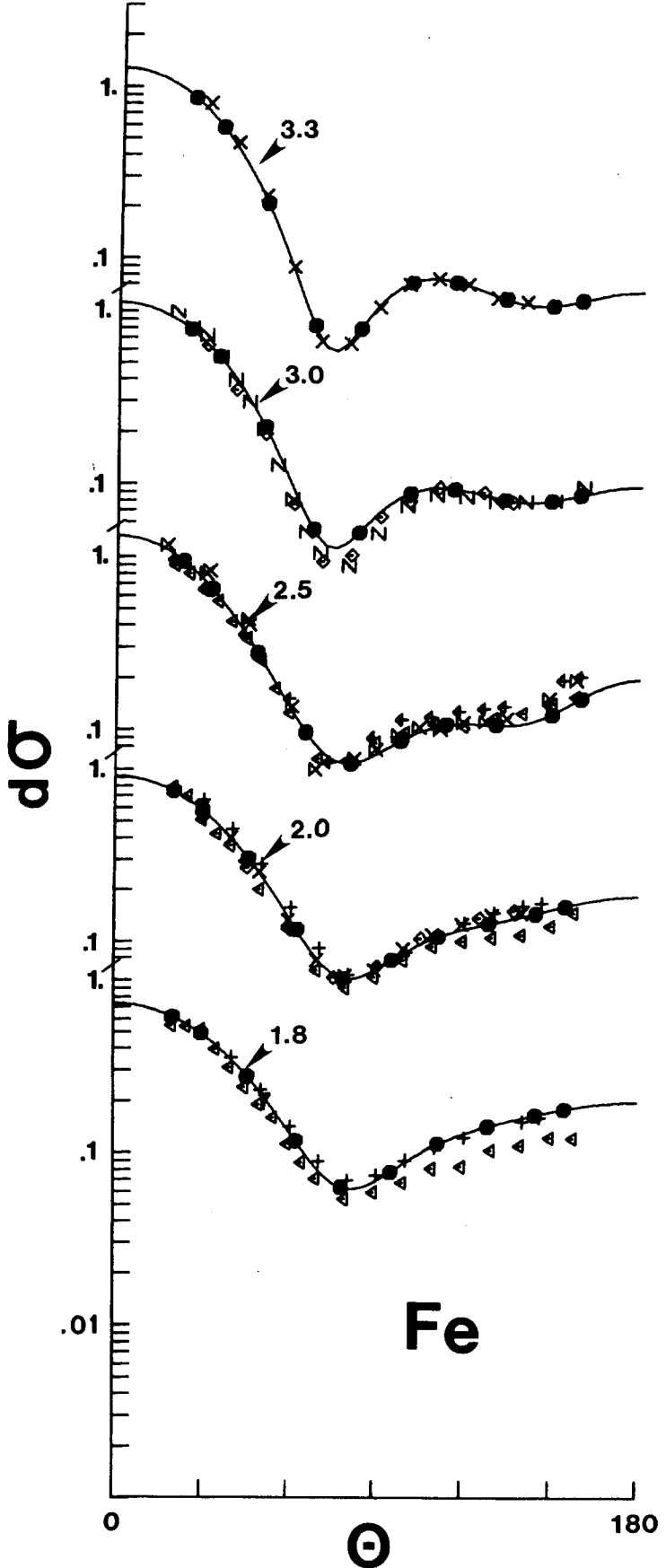


TABLE 1. Observed Inelastic-Neutron Excitations in Elemental Iron

No.	E_x (MeV)	dE_x (MeV)	E_x (MeV) ^a	Isotopic Identification ^a
1	.853	.050	0.847	Fe-56 (2+)
2	1.389	.030	1.407	Fe-54 (2+)
3	2.097	.022	2.085	Fe-56 (4+)
4	2.579	.035	2.539 2.564	Fe-54 (4+) Fe-54 (0+)
5	2.677	.014	2.658	Fe-56 (2+)
6	2.974	.011	2.940 2.960 2.948 2.981	Fe-56 (0+) Fe-56 (2+) Fe-54 (6+) Fe-54 (2+)
7	3.152	.021	3.120 3.123 3.163	Fe-56 Fe-56 Fe-54

^aTaken for Ref. 22.

of similar magnitude. Generally, the cross sections relevant to the lower-energy and prominent excited states (e.g. the 853 keV state) were known to better accuracy.

The observed 853 keV "state" was attributed to the reported 847(2+) keV level in ^{56}Fe . The excitation of this state is a dominant feature of inelastic neutron scattering from iron at the energies of the present experiments. The measured differential cross sections for the excitation of this state, averaged over 200 keV increments, are shown in Fig. 5. As the incident energy increases from ~ 1.7 MeV to 4.0 MeV the distributions change from a general symmetry about 90 deg. to a pronounced forward peaking indicative of a direct-reaction component. The angle-integrated cross sections for the excitation of this state are compared with previously reported measured and evaluated results in Fig. 6. Representative previous measured results are given in Refs. 23 to 32. Most previous measurements were made at isolated incident energies with various resolutions, thus comparisons are seriously perturbed by the large fluctuations. However, the present cross sections tend to be larger than some previously reported values above ~ 2.0 MeV. This could be expected as most previous measurements were at few or single scattering angles often larger than 90 deg. and thus did not include the forward-peaked portion of the distributions. Below ~ 2.0 MeV the present results are in good agreement with comparable averages constructed from the results of Ref. 8 and from the ENDF/B-IV evaluation.⁹ The latter appears to be essentially the good-resolution results of Perey et al.²¹ in this energy range. In addition, there is good agreement with the recent broad-resolution (n;n', γ) results of D. Smith.³³ Generally, the present results indicate an increase in the cross sections for the excitation of the 847 keV level relative to those given ENDF/B-IV above ~ 2.0 MeV.

The observed 1389 keV "state" was attributed to the reported 1407(2+) level in ^{54}Fe . The corresponding angle-integrated cross sections were relatively small as shown in Fig. 6. Above ~ 3.0 MeV the present measurement had to be corrected for a perturbation due to inelastic scattering ($E_x = 853$ keV) of the second and minority neutron component from the source reaction with the consequence of increased cross-section uncertainties. Despite this measurement problem and the small magnitudes of the cross sections the present results are in good agreement with previously reported measured values and with the evaluation of ENDF/B-IV.⁹

The observed 2097 keV "state" was attributed to the reported 2085(4+) level in ^{56}Fe . The present angle-integrated cross sections are in good agreement with a number of previous experimental results and with the evaluation of ENDF/B-IV as illustrated in Fig. 6.

The excitation of a "state" at 2579 keV was observed. It probably consisted of two unresolved components due to the excitation of the reported 2539 and 2564 keV levels in ^{54}Fe . In addition, inelastically scattered neutrons ($E_x = 2085$ keV) from the second neutron group of the source reaction made a major contribution to the observed neutron group. That contribution was so large that corrections could not be reliably

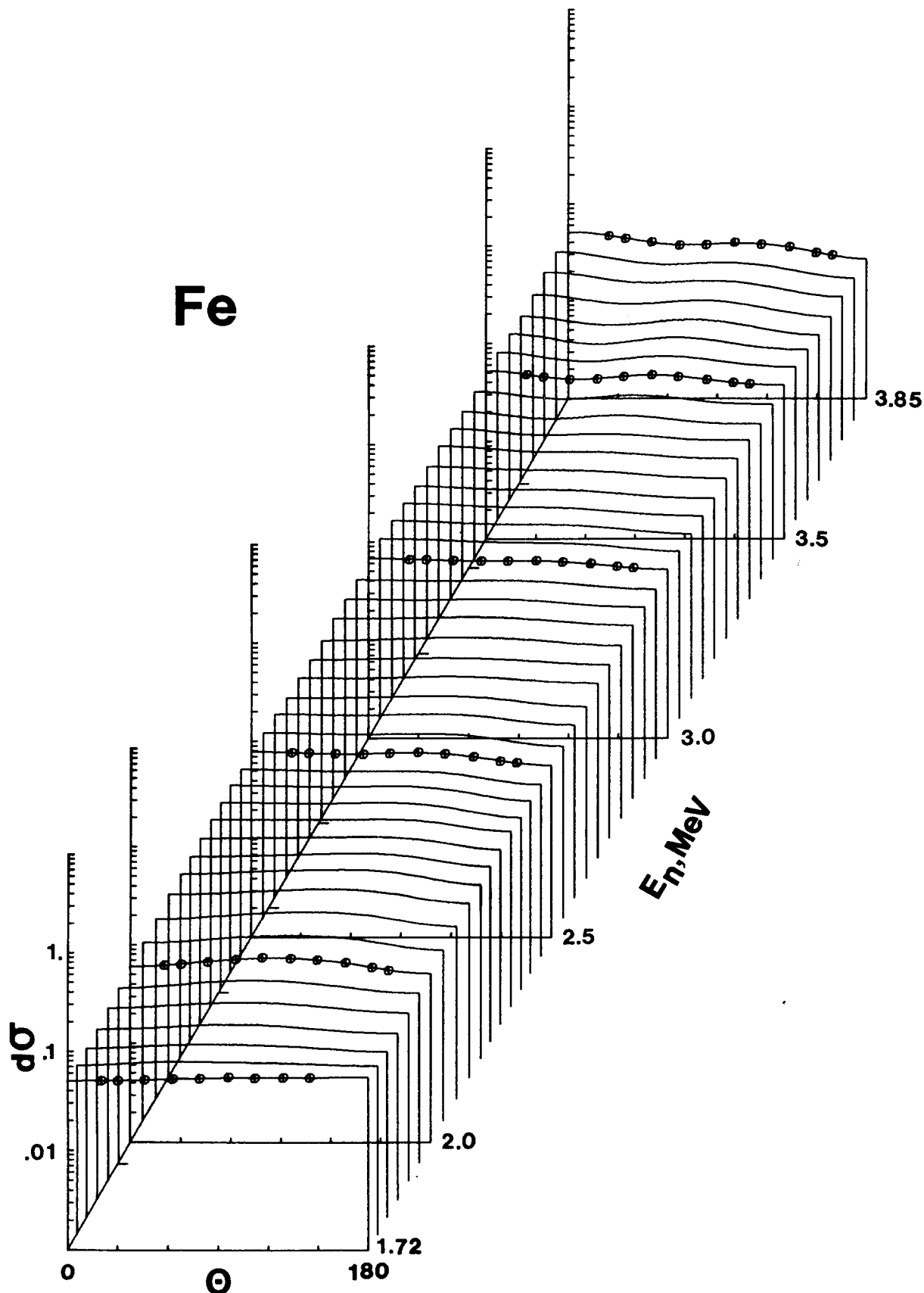


Fig. 5. Measured Differential Cross Sections for the Excitation of the 853 keV State in ^{56}Fe . The notation is identical to that of Fig. 1.

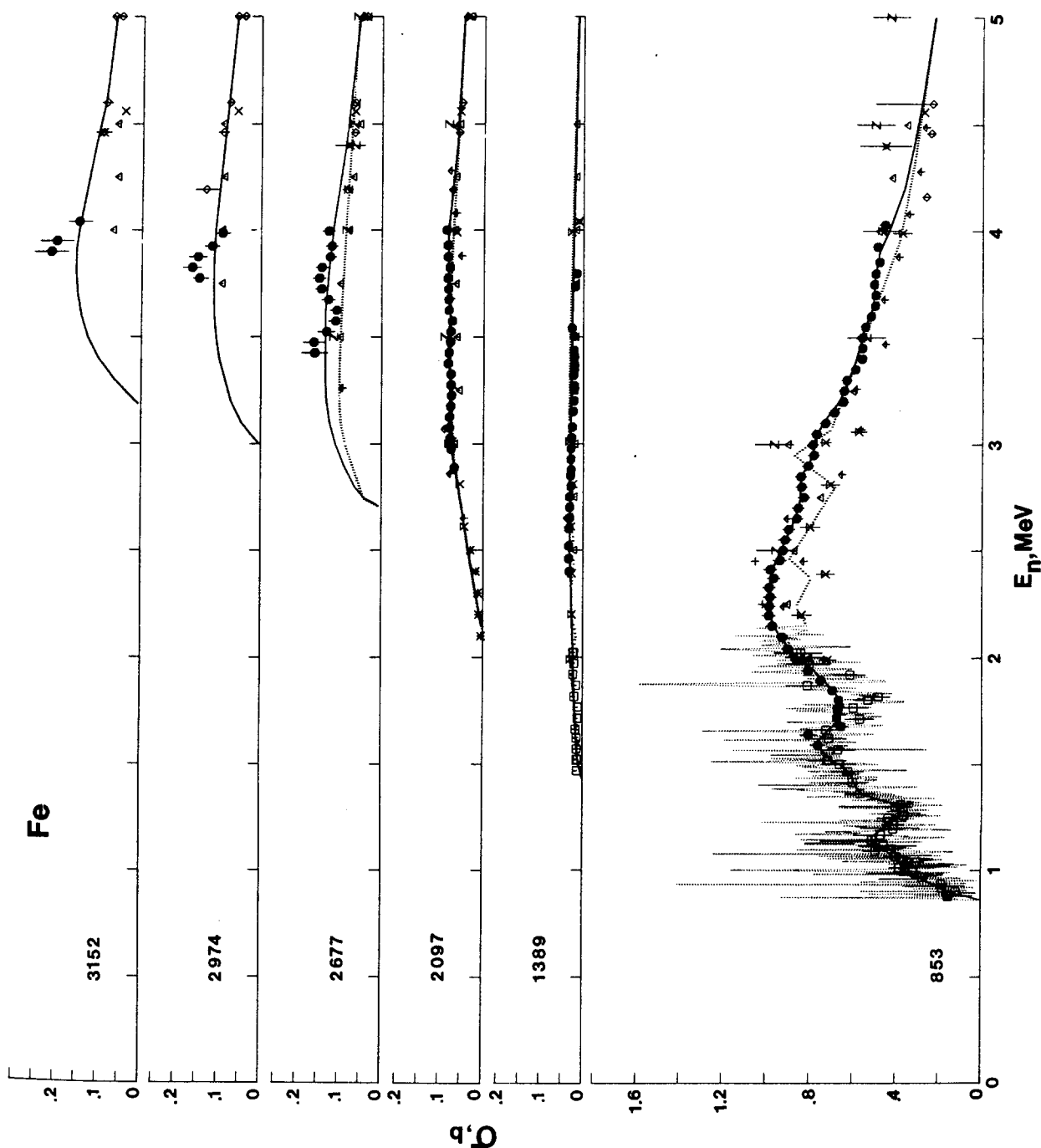


Fig. 6. Measured Inelastic Neutron Excitation Cross Sections of Elemental Iron. The present measured values are indicated by solid data symbols. Other symbols indicate experimental results as defined in the reference list. The solid curve is an "eye-guide" constructed through the present measurements. The dotted curve indicates the respective cross sections as given in ENDF/B-IV. Observed excitation energies are numerically given in keV for each section of the figure.

made and thus cross sections were only qualitatively estimated. They were relatively very small (of the order of 10 mb/sr). Previously reported measurements made with isotopic samples³⁰ indicate that the cross sections for these two states in ^{54}Fe are small (several tens of mb).

The observed excitation of a "state" at 2677 keV was attributed to the reported 2658(2+) keV level in ^{56}Fe . The corresponding angle-integrated cross sections are generally somewhat larger than previously reported measured and evaluated quantities as shown in Fig. 6. This difference may not be real as the present results covered a rather limited energy range and therefore the averaging increment was confined to ~ 100 keV. As a consequence the energy-averaged results shown in Fig. 6 appear to retain some energy-dependent fluctuations.

The observed 2975 keV "state" was attributed to a composite of contributions from reported 2940(0+) ^{56}Fe , 2948(6+) ^{54}Fe , 2960(2+) ^{56}Fe and 2981(2+) ^{54}Fe keV levels. The corresponding cross sections are fairly consistent with previously reported measured results, as illustrated in Fig. 6. Moreover, the averaging increment was only ~ 100 keV and, again, residual fluctuations may remain a distorting factor.

The observed 3152 keV "state" was attributed to reported 3120 and 3123 levels in ^{56}Fe and the 3163 state in ^{54}Fe . The present cross-section results are considerably larger than some previously measured values. It is not clear that the various experimental results correspond to a composite of the same three components thus the comparisons of Fig. 6 may not be valid in all cases.

The above inelastic scattering components very largely determine the inelastic scattering cross section of elemental iron to incident-neutron energies of ~ 3.5 MeV. Their sum should be consistent with the non-elastic cross section derived in Sec. III-B, above. "Eye-guides" were constructed through the measured values as indicated by the curves of Fig. 6. Their sum agreed to within $\sim 5\%$ with the deduced non-elastic cross section shown in Fig. 3. This consistency again suggests that the iron inelastic scattering cross sections as given in ENDF/B-IV are too small at energies above ~ 2.0 MeV.

IV. INTERPRETATION

The applicability of optical-statistical-model concepts to the present experimental results was examined.^{34,35} The application was complicated by the large fluctuations in the measured values, even in the 200 keV averages as illustrated in Figs. 2 and 3. Wider averages are difficult to obtain due to the onset of new inelastic-scattering channels every few hundred keV. Given these problems the model considerations were largely subjective.

The model derivation was essentially based upon the measured neutron differential-elastic-scattering cross sections, averaged over 200 keV, as illustrated in Fig. 2. An optical potential was derived from each measured distribution using six-parameter Xi-square fitting procedures (varying real and imaginary strengths, radii and diffusenesses). It was assumed that the element consisted entirely of ^{56}Fe . Compound-nucleus contributions were calculated using the procedure of Hofmann et al.³⁶ and the excited levels of ^{56}Fe given in Table 1. Higher-energy excitations (above 3.2 MeV) were treated as a continuum distribution using the parameters of Gilbert and Cameron.³⁷ The parameters resulting from these fitting procedures varied widely with energy, reflecting the fluctuations in the measured values. However, a general trend of real-potential parameters emerged and these were fixed for the second fitting procedure which was confined to the two imaginary-potential parameters, strength and diffuseness. The imaginary radius was made equivalent to the real radius. The results of this second fitting procedure better defined the imaginary potential. Finally, some further subjective adjustments were made to improve the description of the neutron total cross section. The resulting parameters are summarized in Table 2. Qualitatively, they are similar to some parameter sets reported in the literature.³⁸ However, it should be made very clear that these parameters describe an energy-average behavior and may not, in the present fluctuating context, describe each experimental result.

The overall agreement of measured and calculated neutron elastic-scattering cross sections is reasonably good as illustrated in Fig. 7. The regions where the two types of results tend to be most divergent are generally correlated with prominent structures in total and elastic-scattering cross sections as illustrated in Fig. 3 (e.g. near 2.5 MeV). Explicit comparisons of measured and calculated differential cross sections at 500 keV intervals are shown in Fig. 8. These comparisons were arbitrarily selected and illustrate both good and poor agreement. Yet more than 80% of the measured values agree with the calculated results to within the experimental uncertainty alone. Again some of the poorest agreement is in the 2.5 MeV region of large fluctuation.

The calculated neutron-total cross sections and a 200 keV average of the measured results of Ref. 6 are in reasonable agreement as illustrated in Fig. 9. This comparison illustrates the unusual phenomenological feature of the potential, an energy dependent diffuseness of the imaginary term. This behavior was suggested by the fitting of elastic-scattering distributions and refined so as to reproduce the experimentally indicated total-cross-section minimum near 1.0 MeV. This pragmatic approach provides a reasonable solution to a long-standing problem in this mass-energy region. The physical implications, if any, are not clear.

The calculated inelastic neutron excitation cross sections are compared with the present experimental values in Fig. 9. The calculations were confined to ^{56}Fe and corrected for the isotopic content of the elemental target. The calculated excitations of the prominent 847 keV (2+) level are generally ~15% smaller than the measured values. In regions of large fluctuations the discrepancy can be larger. Measured and calculated cross sections for the excitation of the 2085 keV (4+) level generally agree to within

TABLE 2. Optical-Model Parameters

Real Strength ^a	$V = 52 - 0.3 \cdot E(\text{MeV}), \text{MeV}$
Real Radius	1.236, F
Real Diffuseness	0.493, F
Imaginary Strength ^b	$W = 10.2 - 0.2 \cdot E(\text{MeV}), \text{MeV}$
Imaginary Radius	1.236, F
Real Diffuseness ^c	0.605, F
Spin-orbit Strength ^d	8 MeV

^aSaxon form.

^bSaxon-derivative form.

^cValue constant from 2.8 to 4.0 MeV and decreasing from 0.605 F at 2.8 MeV to 0.25 F at 1.0 MeV in linear manner.

^dThomas form.

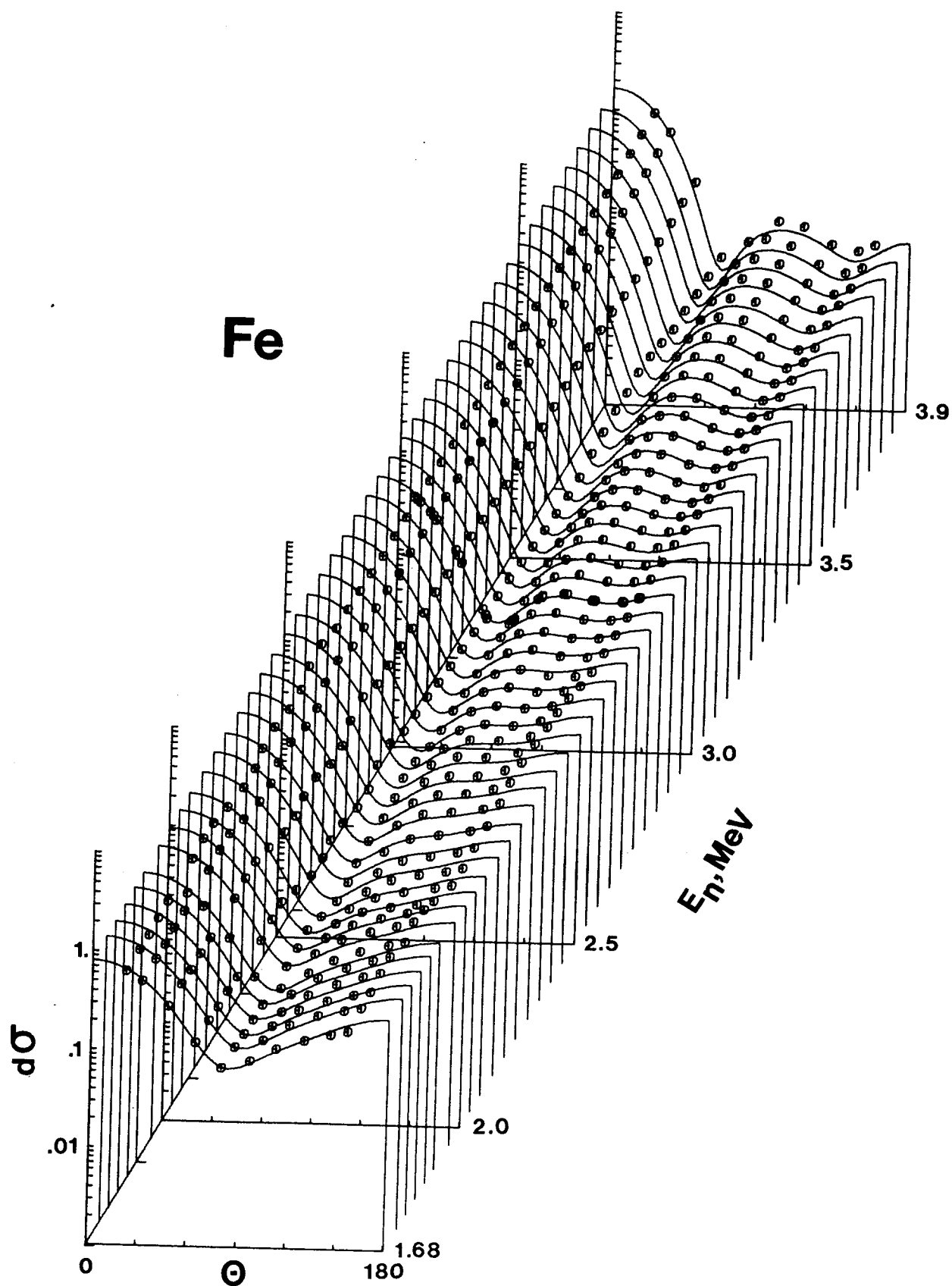
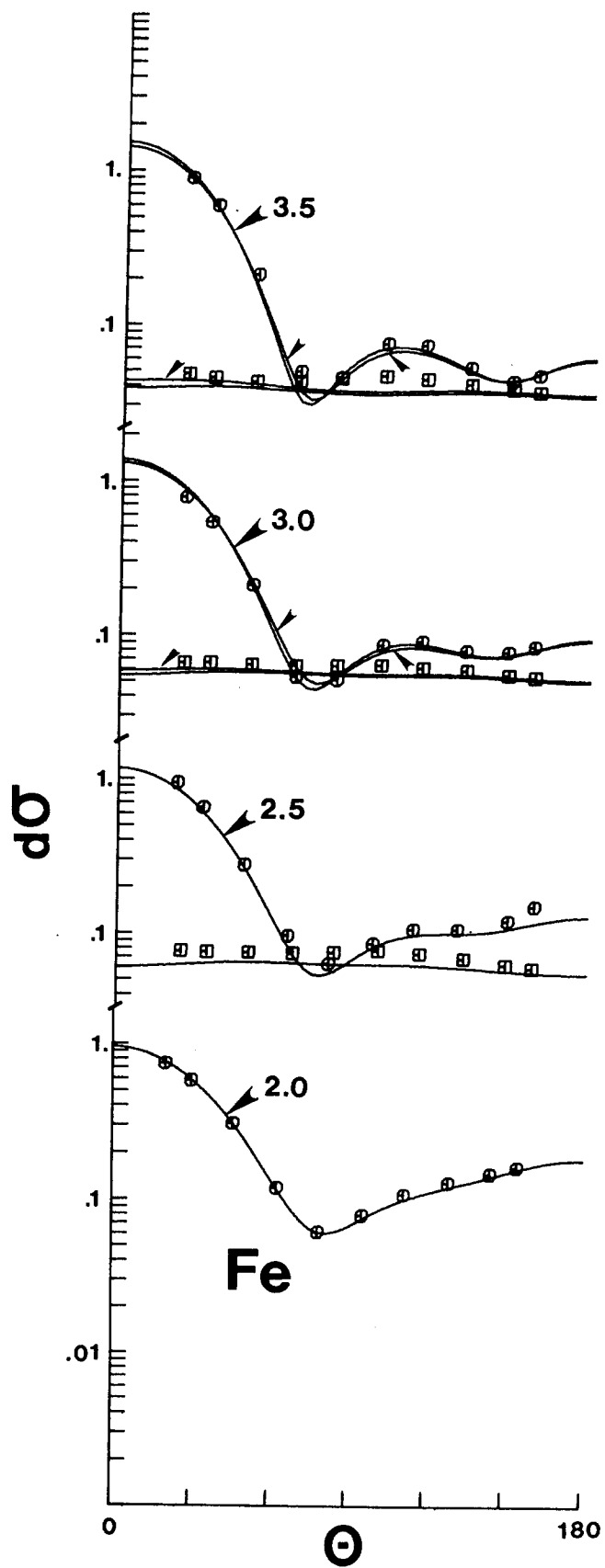


Fig. 7. Comparison of Measured (Data Points) and Calculated (Curves) Differential Elastic Scattering Cross Sections of Elemental Iron. The dimensionality is identical to that of Fig. 1.

Fig. 8. Comparisons of Illustrative Measured and Calculated Differential Scattering Cross Sections of Elemental Iron. Incident neutron energies are noted in MeV. The present experimental results are indicated by data symbols where circular points denote elastic scattering and square points the excitation of the 847 keV level. Simple curves denote the results of spherical calculations and those with "tick" marks results of coupled-channels calculations as described in the text. The dimensionality is identical to that of Fig. 1. (Figure on following page.)



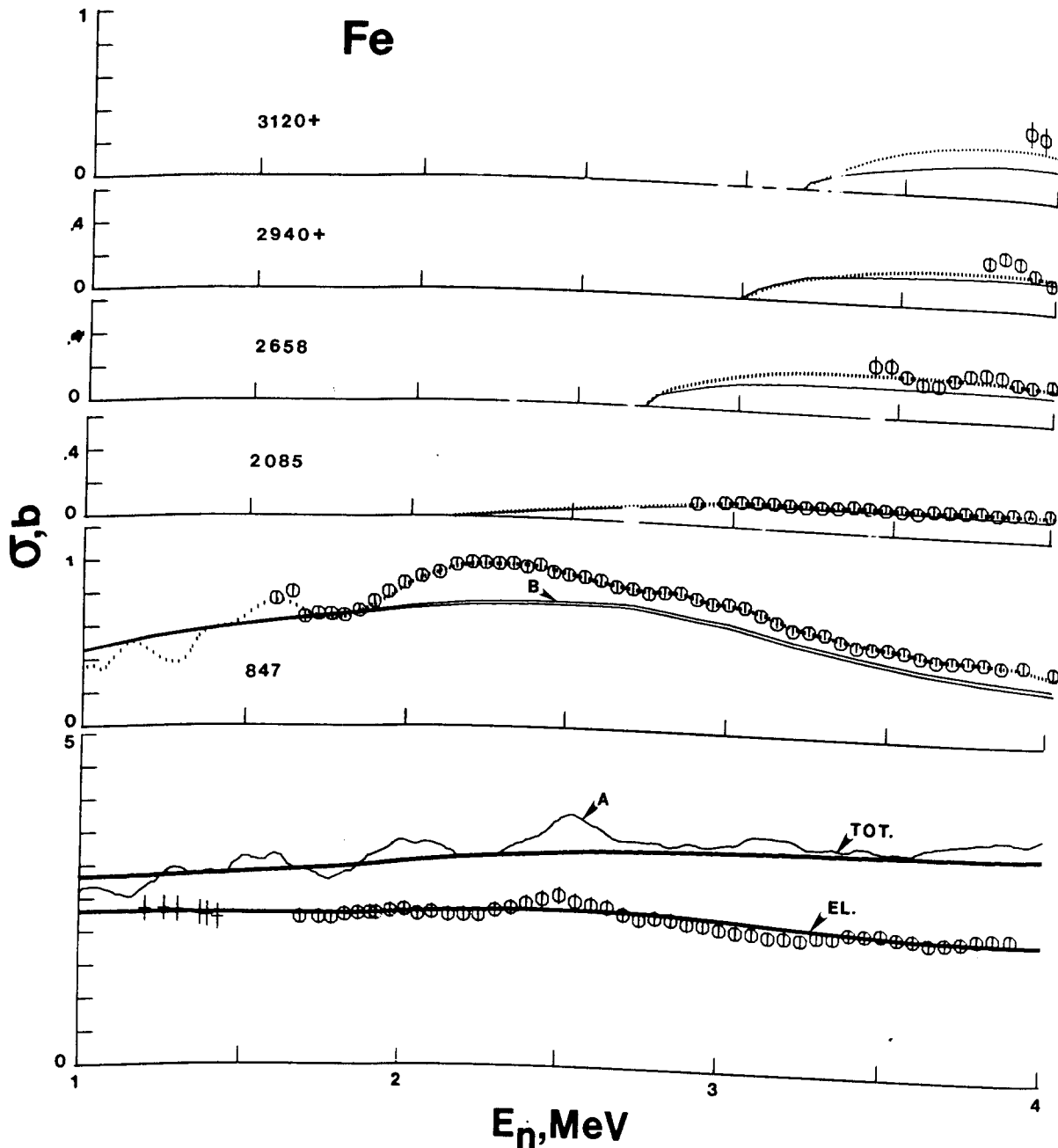


Fig. 9. Comparisons of Measured and Calculated Neutron Cross Sections of Elemental Iron. The present measured values are indicated by circular data points and those of Ref. 8 by crosses. A 200 keV average of the neutron total cross sections of Ref. 6 is indicated by curve "A". Solid curves without notation indicate the results of spherical calculations and the "B" curve the results of coupled-channels calculations as described in the text. The dotted curves are the "eye-guides" of Fig. 6. Excitation energies taken from Ref. 22 and Table 1 are numerically given in keV.

2.

<10%. The measured cross sections for the excitation of the 2658 keV (2+) level appear to fluctuate by rather large amounts but are systematically higher than the calculated values. The calculated excitations of the 2940 + 2960 keV (0+, 2+) composite level are reasonably consistent with the measured values given the limited extent of the latter and some additional contributions from ^{54}Fe not considered in the calculations. The calculated and measured excitations of the composite 3125 keV level are not in very good agreement. This is not surprising as the underlying J- π values are not well known (3+ and 2+ were used in the present calculations) and there are several ^{54}Fe contributions that were not considered in the calculations.

Given the underlying problem of large fluctuations making the average behavior difficult to determine, uncertainties in some J- π values and cumulative contributions from ^{54}Fe the agreement between measured and calculated neutron excitation cross sections was judged acceptable. The largest-magnitude discrepancies are associated with the first (2+) level. Here the calculations are particularly sensitive to the details of the compound-nucleus calculations. The present work employs the formalism of Hofmann et al.³⁶ Relatively small variations within this framework (e.g. variations in the degree of freedom used in estimating level-spacing distributions) can significantly effect the calculated compound-nucleus result. At higher energies the present calculations employed the continuum distributions of Gilbert and Cameron³⁷ to estimate competition from channels above those of the present measurements. This approximation may not be entirely appropriate at the relatively low-energies of the present experiments.

^{56}Fe was assumed to be a vibrational nucleus with the first level (847 keV(2+)) a one-phonon vibrational excitation. This is consistent with the observed tendency of scattered neutrons resulting from the excitation of this level to be somewhat preferentially distributed toward forward scattering angles (see Fig. 5). The magnitudes of such direct-vibrational excitations were assessed using the potential of Table 2 in a coupled-channels calculation. The deformation was taken from the tabulation of Stelson and Grodzins;³⁹ i.e. $\beta_2 = 0.25$. Using this simple approach, the calculated contributions of direct-vibrational excitations to the cross sections for the excitation of the 847 keV level were small, as shown in Fig. 9, but they did improve the agreement with the measured values. The direct-vibrational component also produced a forward-angle bias to the differential-inelastic-scattering cross sections which was in better agreement with experimental data as illustrated in Fig. 8. The vibrational coupling of ground and first-excited levels also significantly altered the calculated elastic-scattering distributions as shown in Fig. 8. Subsequent potential-parameter selection within the context of the vibrational model was not pursued as the fluctuations probably remain the dominant sources of uncertainty. However, the results of Ref. 40 suggest that such procedures would result in increased calculated cross sections for the excitation of the 847 keV state and thus improved agreement with the measured values.

V. EVALUATED SCATTERING CROSS SECTIONS

The objective of the present evaluation was the provision of evaluated-neutron-scattering cross sections of elemental iron in the limited energy scope of 1.0 to 4.0 MeV. An intermediate energy resolution of 200 keV was selected as most appropriate in this transitional-energy region between well resolved resonance structure and a smooth energy-dependence of the cross sections. This evaluation and all comparisons with other results are in the context of this 200 keV resolution function. The present evaluation should be reasonably descriptive of broad intermediate-resonance structure and relatively free of undue perturbations from single or a few large resonances. It is hoped that the present evaluation will find use either as a subset of more comprehensive evaluation efforts or in the verification of evaluations undertaken under other auspices. The numerical values of the present evaluation are given in the ENDF/B format in the Appendix.⁹

A. Evaluated Neutron-Elastic-Scattering Cross Sections

At energies above 1.5 MeV the evaluated elastic scattering cross sections were taken from the present measured values following the "eye-guide" of Fig. 3. Below 1.5 MeV the evaluation follows the same "eye-guide" which is based upon the measured values of Ref. 8 and a fluctuating shape consistent with the neutron-total cross sections of Ref. 6 and the elastic scattering cross sections of Ref. 21. The uncertainties associated with the present evaluated results are believed to be less than 5% above 1.5 MeV and possibly somewhat larger at the lower energies, below those of the present measurements.

The evaluated relative neutron-differential-elastic-scattering distributions at energies above 1.5 MeV were taken directly from the present measurements (see Fig. 2). At energies of less than 1.5 MeV, 200 keV averages were constructed from the measured values of Ref. 21. The evaluated results were not directly dependent upon the absolute normalizations of the two measured data sets involved. Generally, other previously reported measured differential scattering results were obtained at isolated energies and subject to local fluctuations. Thus they were not quantitatively considered in the evaluation.

The final evaluated neutron-differential-elastic-scattering cross sections are summarized in Fig. 10.

B. Evaluated Neutron-Inelastic-Scattering Cross Sections

The present inelastic-scattering evaluation considers levels up to excitations of 3.2 MeV as generally defined in Table 1. The evaluation directly follows the "eye-guides" of Fig. 6. That figure relates the evaluation to the present measurements and the body of previously reported experimental information.

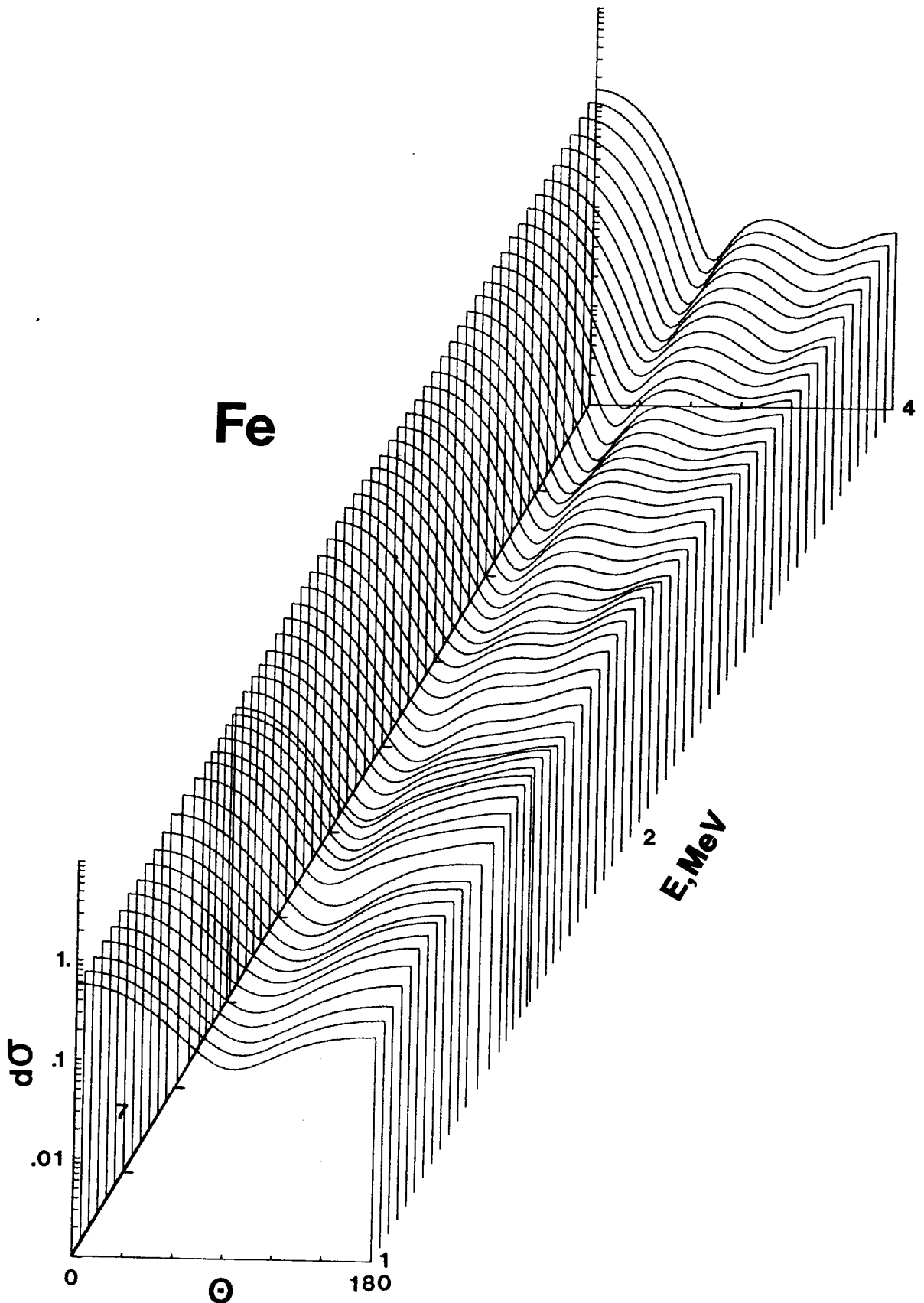


Fig. 10. Outline of Evaluated Differential Elastic Scattering Cross Sections of Elemental Iron. The dimensionality is identical to that of Fig. 1.

The excitation of the 847 keV (^{56}Fe , 2+) state below 1.6 MeV follows the systematic and broad-resolution (n;n', γ) results of Smith.³³ The latter have been shown to be consistent with both the present direct neutron measurements and the high-resolution results of Perey et al.²¹ in the region of energy overlap. Above 1.6 MeV the evaluation follows the present measurements which are consistent with a number of previously reported energy-isolated results; e.g. Cranberg and Levin,²³ Hopkins and Silbert,²⁴ Lindlow,²⁵ and Tsukada et al.²⁶ In the context of the broad 200 keV resolution, the present evaluation is believed known to within $\sim 5\%$.

The excitation of the 1.408 MeV level was attributed entirely to the 2+ state in ^{54}Fe . The present measured values give good definition between 2.4 and 4.0 MeV and are extended to threshold using the results of Smith.³³ The present evaluation is consistent with a number of previously reported measured values and with calculational estimates based upon the potential of Table 2. The uncertainties associated with the evaluation are $\sim 10\%$ to 20%. These relatively large uncertainties are of little concern in most applications as the cross-section magnitudes are small.

The evaluation for the 2.085 MeV (^{56}Fe , 4+) follows the present measurements and extends to threshold via the results of Gilboy and Towle²⁷ and of Tucker et al.²⁸ The general data base is very consistent and thus the evaluation is believed known to better than 10% throughout the region of appreciable cross sections.

The evaluation includes the excitation of a level at 2.539 (two components from ^{54}Fe) for completeness. The present measurements give a qualitative indication of the cross section magnitudes that is consistent with the isotopic results of Lindlow.²⁵ and with calculational estimates. Therefore, the calculations were used for the evaluation. The associated uncertainties maybe relatively large but the cross section magnitudes are very small and thus will have little effect in most applications.

The evaluation for the excitation of the 2.658 MeV (^{56}Fe , 2+) level is based upon a relative calculated energy-dependent shape normalized to the present experimental values. The evaluation reasonably extrapolates to the higher-energy experimental results of Lindlow.²⁵ and of Kinney and Perey.²⁹ However, below 4.0 MeV the evaluation is somewhat larger than some previously reported values. This may be the result of the limited energy range of the present measurements which made it difficult to accurately determine the energy-averaged magnitudes. Despite these problems, the evaluation uncertainties were estimated to be $\sim 15\%$.

The evaluations for the excitation of 2.940 and 3.120 MeV levels were obtained by normalizing calculated excitation functions to the few measured values of the present work. The calculations involved only ^{56}Fe and both observed levels certainly contain ^{54}Fe components. Moreover, both levels consist of at least two ^{56}Fe components and the J- π values involved in the 3.125 MeV "level" are not certain. All of these factors contribute to evaluation uncertainties which are estimated to be 10 to 20%. These are probably very conservative estimates as the present evaluation

is in very good agreement with previously reported measured cross sections for the excitation of the 2.940 MeV level and reasonably consistent with those reported by Lindlow,²⁵ and by Kinney and Perey²⁹ for the excitation of the 3.125 level.

The above individual components of the evaluation were summed to obtain the total neutron-inelastic-scattering cross sections shown in Fig. 11. The result is in very good agreement with the non-elastic-scattering cross sections derived above. Several non-scattering channels are open in this energy range but the corresponding cross sections are too small to significantly influence these comparisons. The estimated uncertainty in the derived total-neutron-inelastic-scattering cross section was estimated to be 5% to ~ 3.3 MeV. Above 3.3 MeV additional scattering channels are open that were not observed in the present experiments. Fig. 11 suggests that the cumulative sum of their cross sections is $\sim 200 \pm 75$ mb at 4.0 MeV. That appears to be a reasonable value in view of the results of higher-energy measurements by Kinney and Perey.²⁹

As noted above, the observed angular distributions of neutrons resulting from the inelastic excitation of the above states were essentially isotropic. An exception is the excitation of the 847 keV state. Therefore, the evaluation uses the measured neutron angular distributions of Fig. 5 for the 847 keV state and accepts isotropy for all other inelastic-neutron angular distributions.

Between approximately 2.1 and 3.5 MeV the present evaluated inelastic neutron scattering cross sections are 10 to 20% larger than the corresponding quantities given in ENDF/B-IV. The major contribution to this increase is the excitation of the 847 keV level. Changes of this magnitude are not insignificant in the context of fast fission reactors. For example, they reflect $\sim 0.15\%$ variations in the k_{eff} of a representative LMFBR system and the effect can rapidly increase with iron content (e.g. in FTF systems).⁴¹

VI. SUMMARY REMARKS

Differential neutron-scattering cross sections of elemental iron were measured in sufficient detail to well define the differential broad-resolution elastic and inelastic scattering cross sections from 1.5 to 4.0 MeV. The results portray intermediate-resonance structure having periodicities and widths of several hundred keV. The elastic-scattering cross sections, determined to accuracies of $\sim 5\%$, together with reported neutron-total cross sections imply a non-elastic cross section to accuracies of $\sim 5\%$. This non-elastic cross section is consistent with the results of concurrently measured neutron-inelastic-excitation cross sections. Both the implied non-elastic cross sections and the directly measured inelastic scattering cross sections are significantly larger in magnitude than comparable values given in ENDF/B-IV over wide energy regions. The consequence is a significant impact upon the results of LMFBR neutronic calculations. Optical-statistical model calculations led to results generally consistent with the measured values. However, strong fluctuations in this mass-energy region make explicit model fits to individual measured

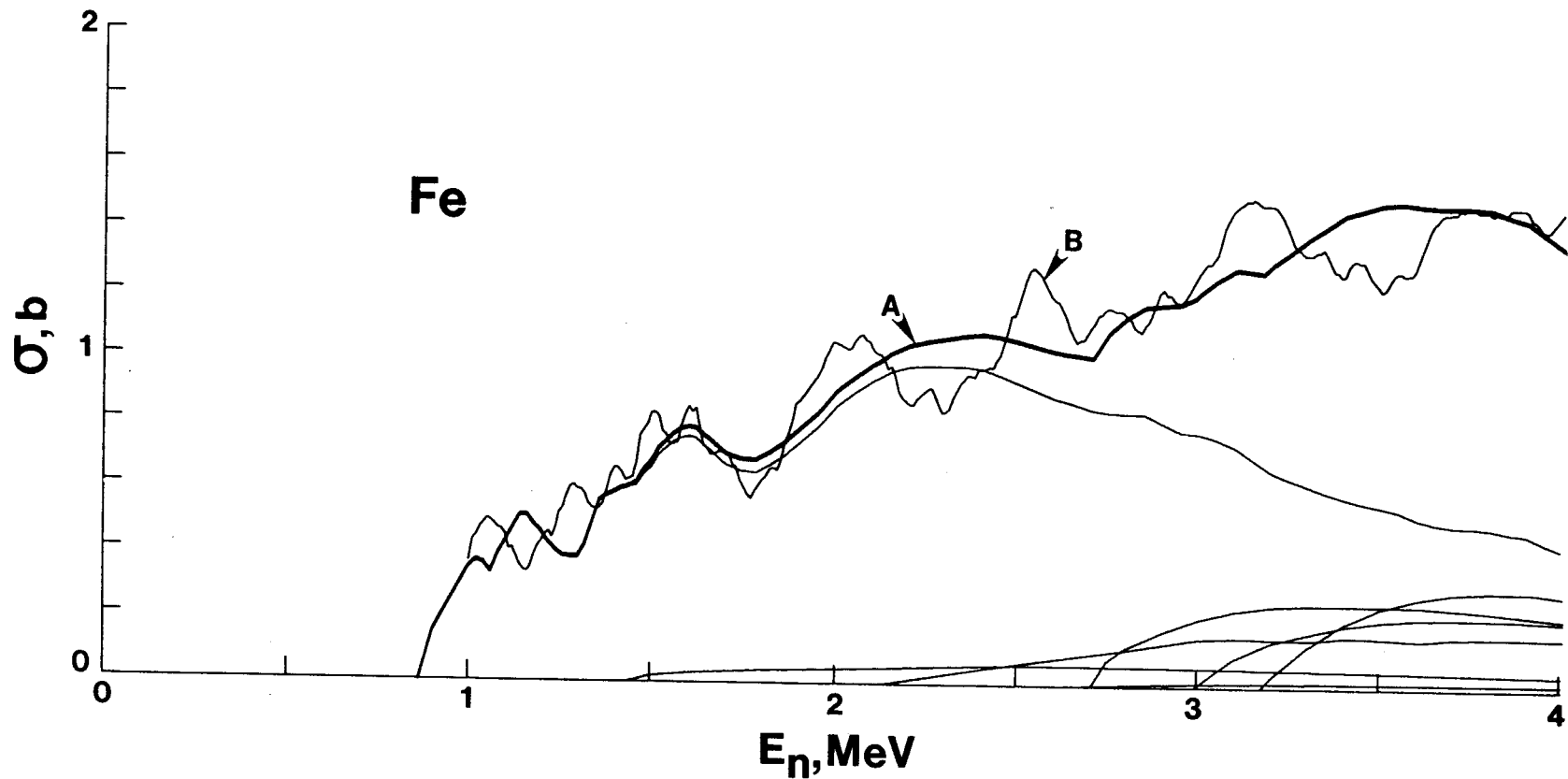


Fig. 11. Summary of Evaluated Neutron Inelastic Excitation Cross Sections of Elemental Iron. Simple curves indicate the individual components as defined in Table 1 and the Appendix. Curve "B" indicates the non-elastic cross section as derived from the present measurements and the neutron total cross sections of Ref. 6. Curve "A" is the sum of the individual inelastic excitation cross sections.

distributions of little, if any, significance. Only comparisons in a wide energy average are meaningful. Despite their scope and detail, it was not clear that the present measurements provided a good definition of the energy-average behavior requisite to energy-averaged model interpretations. The model interpretations are further complicated by direct-vibrational interactions. Such processes are suggested by the anisotropy of some of the measured differential inelastically-scattered neutron distributions and significantly influence the interpretation of the neutron elastic scattering processes.

APPENDIX

2.60000+ 4 5,53650+ 1 0 0 0 1 26 0 0
 0.0 0,0 0 0 0 0 26 1451
 0.0 0,0 0 0 4 0 26 1451
 ----- 17 26 1451

EVALUATED NEUTRON SCATTERING CROSS SECTIONS OF IRON, 1-4 MEV,
 DOCUMENTED IN ANL/NDM-47(1979),

1	451	24	1	26	1451
3	2	24	1	26	1451
3	51	31	1	26	1451
3	52	6	1	26	1451
3	53	8	1	26	1451
3	54	6	1	26	1451
3	55	7	1	26	1451
3	56	7	1	26	1451
3	57	7	1	26	1451
4	2	127	1	26	1451
4	51	99	1	26	1451
4	52	2	1	26	1451
4	53	2	1	26	1451
4	54	2	1	26	1451
4	55	2	1	26	1451
4	56	2	1	26	1451
4	57	2	1	26	1451

2.60000+ 4 5,53650+ 1 0 99 0 0 26 1 0
 0.0 0,0 0 0 1 61 26 0 0
 61 2 26 3 2
 26 3 2

.10000E 07	.22500E 01	.10500E 07	.21800E 01	.11000E 07	.21500E 01	26 3 2
.11500E 07	.21800E 01	.12000E 07	.22500E 01	.12500E 07	.23500E 01	26 3 2
.13000E 07	.23700E 01	.13500E 07	.23300E 01	.14000E 07	.22600E 01	26 3 2
.14500E 07	.22300E 01	.15000E 07	.23000E 01	.15500E 07	.23500E 01	26 3 2
.16000E 07	.23300E 01	.16500E 07	.22700E 01	.17000E 07	.22200E 01	26 3 2
.17500E 07	.22200E 01	.18000E 07	.22350E 01	.18500E 07	.22750E 01	26 3 2
.19000E 07	.22900E 01	.19500E 07	.23100E 01	.20000E 07	.23400E 01	26 3 2
.20500E 07	.22700E 01	.21000E 07	.23000E 01	.21500E 07	.22600E 01	26 3 2
.22000E 07	.22600E 01	.22500E 07	.22600E 01	.23000E 07	.23400E 01	26 3 2
.23500E 07	.23800E 01	.24000E 07	.24500E 01	.24500E 07	.25200E 01	26 3 2
.25000E 07	.25800E 01	.25500E 07	.24900E 01	.26000E 07	.24500E 01	26 3 2
.26500E 07	.24200E 01	.27000E 07	.23200E 01	.27500E 07	.22500E 01	26 3 2
.28000E 07	.22800E 01	.28500E 07	.22600E 01	.29000E 07	.22100E 01	26 3 2
.29500E 07	.22000E 01	.30000E 07	.21500E 01	.30500E 07	.21200E 01	26 3 2
.31000E 07	.21100E 01	.31500E 07	.20700E 01	.32000E 07	.20700E 01	26 3 2
.32500E 07	.20500E 01	.33000E 07	.21000E 01	.33500E 07	.21000E 01	26 3 2
.34000E 07	.21700E 01	.34500E 07	.21600E 01	.35000E 07	.21800E 01	26 3 2
.35500E 07	.21300E 01	.36000E 07	.21200E 01	.36500E 07	.20700E 01	26 3 2
.37000E 07	.20900E 01	.37500E 07	.21100E 01	.38000E 07	.21600E 01	26 3 2
.38500E 07	.21800E 01	.39000E 07	.21800E 01	.39500E 07	.22000E 01	26 3 2
.40000E 07	.22300E 01	.00000E 00	.00000E 00	.00000E 00	.00000E 00	26 3 2

2.60000+ 4 5,53620+ 1 0 1 0 0 26 3 0
 0.0 -8,46770+ 5 0 0 1 83 26 3 51
 83 2 26 3 51
 .10000E 07 .35000E 00 .10200E 07 .37000E 00 .10400E 07 .36000E 00 26 3 51
 .10600E 07 .33300E 00 .10800E 07 .39000E 00 .11000E 07 .43000E 00 26 3 51
 .11200E 07 .47000E 00 .11400E 07 .51000E 00 .11600E 07 .51000E 00 26 3 51
 .11800E 07 .48000E 00 .12000E 07 .45800E 00 .12200E 07 .42500E 00 26 3 51
 .12400E 07 .40100E 00 .12600E 07 .38400E 00 .12800E 07 .38100E 00 26 3 51

.13000E 07	.38200E 00	.13200E 07	.42000E 00	.13400E 07	.49000E 00	26	3	51	60
.13600E 07	.55800E 00	.13800E 07	.57500E 00	.14000E 07	.58500E 00	26	3	51	61
.14200E 07	.59700E 00	.14400E 07	.60200E 00	.14600E 07	.60600E 00	26	3	51	62
.14800E 07	.64000E 00	.15000E 07	.66000E 00	.15200E 07	.70000E 00	26	3	51	63
.15400E 07	.72000E 00	.15600E 07	.74000E 00	.15800E 07	.75300E 00	26	3	51	64
.16000E 07	.75700E 00	.16200E 07	.75000E 00	.16400E 07	.73000E 00	26	3	51	65
.16600E 07	.71200E 00	.16800E 07	.69000E 00	.17000E 07	.67000E 00	26	3	51	66
.17400E 07	.65000E 00	.17800E 07	.64500E 00	.18200E 07	.67000E 00	26	3	51	67
.18600E 07	.70000E 00	.19000E 07	.74000E 00	.19500E 07	.78800E 00	26	3	51	68
.20000E 07	.85500E 00	.20500E 07	.89700E 00	.21000E 07	.93500E 00	26	3	51	69
.21500E 07	.96500E 00	.22000E 07	.98000E 00	.22500E 07	.98300E 00	26	3	51	70
.23000E 07	.98100E 00	.23500E 07	.98000E 00	.24000E 07	.97300E 00	26	3	51	71
.24500E 07	.95300E 00	.25000E 07	.93000E 00	.25500E 07	.90700E 00	26	3	51	72
.26000E 07	.88500E 00	.26500E 07	.86800E 00	.27000E 07	.85000E 00	26	3	51	73
.27500E 07	.84100E 00	.28000E 07	.84000E 00	.28500E 07	.83900E 00	26	3	51	74
.29000E 07	.81000E 00	.29500E 07	.78400E 00	.30000E 07	.78000E 00	26	3	51	75
.30500E 07	.76300E 00	.31000E 07	.74000E 00	.31500E 07	.70200E 00	26	3	51	76
.32000E 07	.66500E 00	.32500E 07	.64100E 00	.33000E 07	.62100E 00	26	3	51	77
.33500E 07	.60100E 00	.34000E 07	.58400E 00	.34500E 07	.57000E 00	26	3	51	78
.35000E 07	.55800E 00	.35500E 07	.54600E 00	.36000E 07	.52300E 00	26	3	51	79
.36500E 07	.50800E 00	.37000E 07	.50200E 00	.37500E 07	.50000E 00	26	3	51	80
.38000E 07	.49600E 00	.38500E 07	.48500E 00	.39000E 07	.47800E 00	26	3	51	81
.39500E 07	.45500E 00	.40000E 07	.43300E 00	.00000E 00	.00000E 00	26	3	51	82
2.60000+ 4	5.53620+ 1	0	2	0	0	26	3	0	83
0.0	-1.40800+ 6	0	0	1	8	26	3	52	84
8	2					26	3	52	85
.14340E 07	.00000E 00	.15000E 07	.20000E-01	.16000E 07	.30000E-01	26	3	52	86
.18000E 07	.40000E-01	.20000E 07	.46000E-01	.25000E 07	.63000E-01	26	3	52	87
.30000E 07	.58000E-01	.40000E 07	.43000E-01	.00000E 00	.00000E 00	26	3	52	88
2.60000+ 4	5.53620+ 1	0	3	0	0	26	3	0	89
0.0	-2.08480+ 6	0	0	1	15	26	3	53	90
15	2					26	3	53	91
.21220E 07	.00000E 00	.24000E 07	.50000E-01	.26000E 07	.83000E-01	26	3	53	92
.28000E 07	.11500E 00	.30000E 07	.15000E 00	.31000E 07	.15500E 00	26	3	53	93
.32000E 07	.15000E 00	.33000E 07	.14800E 00	.34000E 07	.16000E 00	26	3	53	94
.35000E 07	.15600E 00	.36000E 07	.15000E 00	.37000E 07	.16000E 00	26	3	53	95
.38000E 07	.16100E 00	.39000E 07	.16000E 00	.40000E 07	.15800E 00	26	3	53	96
2.60000+ 4	5.53620+ 1	0	4	0	0	26	3	0	97
0.0	-2.58780+ 6	0	0	1	8	26	3	54	98
8	2					26	3	54	99
.26340E 07	.00000E 00	.28000E 07	.70000E-02	.30000E 07	.13000E-01	26	3	54	100
.32000E 07	.16000E-01	.34000E 07	.17000E-01	.36000E 07	.17800E-01	26	3	54	101
.38000E 07	.17600E-01	.40000E 07	.17200E-01	.00000E 00	.00000E 00	26	3	54	102
2.60000+ 4	5.53620+ 1	0	5	0	0	26	3	0	103
0.0	-2.65750+ 6	0	0	1	12	26	3	55	104
12	2					26	3	55	105
.27050E 07	.00000E 00	.27500E 07	.80000E-01	.28000E 07	.12000E 00	26	3	55	106
.29000E 07	.17000E 00	.30000E 07	.21000E 00	.31000E 07	.23700E 00	26	3	55	107
.32000E 07	.25300E 00	.33000E 07	.25800E 00	.34000E 07	.25800E 00	26	3	55	108
.36000E 07	.25600E 00	.38000E 07	.24000E 00	.40000E 07	.21900E 00	26	3	55	109
2.60000+ 4	5.53620+ 1	0	6	0	0	26	3	0	110
0.0	-2.94050+ 6	0	0	1	11	26	3	56	111
11	2					26	3	56	112
.29930E 07	.00000E 00	.30500E 07	.50000E-01	.31000E 07	.90000E-01	26	3	56	113
.32000E 07	.14000E 00	.33000E 07	.16800E 00	.34000E 07	.19500E 00	26	3	56	114
.32000E 07	.14000E 00	.33000E 07	.16800E 00	.34000E 07	.19500E 00	26	3	56	115
.32000E 07	.14000E 00	.33000E 07	.16800E 00	.34000E 07	.19500E 00	26	3	56	116
.32000E 07	.14000E 00	.33000E 07	.16800E 00	.34000E 07	.19500E 00	26	3	56	117
.32000E 07	.14000E 00	.33000E 07	.16800E 00	.34000E 07	.19500E 00	26	3	56	118
.32000E 07	.14000E 00	.33000E 07	.16800E 00	.34000E 07	.19500E 00	26	3	56	119

.35000E 07	.21000E 00	.36000E 07	.21900E 00	.37000E 07	.22000E 00	26	3	56	120
.38000E 07	.22000E 00	.40000E 07	.21000E 00	.00000E 00	.00000E 00	26	3	56	121
						26	3	0	122
2.60000+ 4	5.53620+ 1	0	7	0	0	26	3	57	123
0.0	-3.12070+ 6	0	0	1	10	26	3	57	124
	10	2				26	3	57	125
.31760E 07	.00000E 00	.32000E 07	.30000E-01	.33000E 07	.12500E 00	26	3	57	126
.34000E 07	.20000E 00	.35000E 07	.25000E 00	.36000E 07	.28000E 00	26	3	57	127
.37000E 07	.29800E 00	.38000E 07	.30500E 00	.39000E 07	.30400E 00	26	3	57	128
.40000E 07	.29000E 00	.00000E 00	.00000E 00	.00000E 00	.00000E 00	26	3	57	129
						26	3	0	130
						26	0	0	131
2.60000+ 4	5.53650+ 1	0	1	0	0	26	4	2	132
0.0	5.53650+ 1	0	1	1	62	26	4	2	133
	62	2				26	4	2	134
.00000E 00	.10000E 07	0	0	6	0	26	4	2	135
.24733E 00	.21600E 00	.48714E-01	.51222E- 2	.19273E-02	.76923E-04	26	4	2	136
.00000E 00	.10500E 07	0	0	6	0	26	4	2	137
.22500E 00	.21600E 00	.47857E-01	.66222E-02	.19273E-02	.76923E-04	26	4	2	138
.00000E 00	.11000E 07	0	0	6	0	26	4	2	139
.22167E 00	.22200E 00	.49143E-01	.71667E-02	.20182E-02	.76923E-04	26	4	2	140
.00000E 00	.11500E 07	0	0	6	0	26	4	2	141
.19267E 00	.23200E 00	.55286E-01	.14889E-01	.20000E-02	.76923E-05	26	4	2	142
.00000E 00	.12000E 07	0	0	5	0	26	4	2	143
.15367E 00	.23800E 00	.58143E-01	.18333E-01	.35636E-02	.00000E 00	26	4	2	144
.00000E 00	.12500E 07	0	0	5	0	26	4	2	145
.15467E 00	.24000E 00	.53286E-01	.20333E-01	.40364E-02	.00000E 00	26	4	2	146
.00000E 00	.13000E 07	0	0	6	0	26	4	2	147
.19067E 00	.24800E 00	.56000E-01	.22333E-01	.37364E-02	.76923E-04	26	4	2	148
.00000E 00	.13500E 07	0	0	6	0	26	4	2	149
.18767E 00	.25400E 00	.57286E-01	.19889E-01	.46727E-02	.76923E-04	26	4	2	150
.00000E 00	.14000E 07	0	0	6	0	26	4	2	151
.24100E 00	.26400E 00	.68286E-01	.20333E-01	.48455E-02	.76923E-04	26	4	2	152
.00000E 00	.14500E 07	0	0	6	0	26	4	2	153
.23167E 00	.27200E 00	.74143E-01	.18778E-01	.50364E-02	.76923E-04	26	4	2	154
.00000E 00	.15000E 07	0	0	6	0	26	4	2	155
.24700E 00	.27800E 00	.81857E-01	.18778E-01	.66727E-02	.76923E-04	26	4	2	156
.00000E 00	.15500E 07	0	0	6	0	26	4	2	157
.31100E 00	.28800E 00	.87143E-01	.18889E-01	.74818E-02	.76923E-04	26	4	2	158
.00000E 00	.16140E 07	0	0	6	0	26	4	2	159
.31100E 00	.29200E 00	.97000E-01	.25000E-01	.85545E-02	.76923E-04	26	4	2	160
.00000E 00	.16840E 07	0	0	6	0	26	4	2	161
.27300E 00	.28000E 00	.11471E 00	.31111E-01-	.84727E-03-	.46462E-03	26	4	2	162
.00000E 00	.17430E 07	0	0	6	0	26	4	2	163
.25933E 00	.28000E 00	.11414E 00	.25778E-01	.44636E-03	.37462E-03	26	4	2	164
.00000E 00	.17820E 07	0	0	6	0	26	4	2	165
.25267E 00	.28400E 00	.11357E 00	.27333E-01-	.40818E-03-	.53692E-04	26	4	2	166
.00000E 00	.18230E 07	0	0	6	0	26	4	2	167
.25033E 00	.29600E 00	.11229E 00	.28778E-01-	.39636E-03-	.21615E-03	26	4	2	168
.00000E 00	.18650E 07	0	0	6	0	26	4	2	169
.25067E 00	.30000E 00	.11843E 00	.32778E-01	.47364E-04-	.31154E-03	26	4	2	170
.00000E 00	.19020E 07	0	0	6	0	26	4	2	171
.24900E 00	.29400E 00	.12043E 00	.32333E-01-	.21909E-02-	.26692E-02	26	4	2	172
.00000E 00	.19220E 07	0	0	6	0	26	4	2	173
.25167E 00	.29800E 00	.12329E 00	.39778E-01	.15909E-03	.31846E-03	26	4	2	174
.00000E 00	.19670E 07	0	0	6	0	26	4	2	175
.28167E 00	.30800E 00	.13543E 00	.44222E-01	.10182E-02	.69231E-03	26	4	2	176
.00000E 00	.20130E 07	0	0	6	0	26	4	2	177
.32467E 00	.31200E 00	.13900E 00	.43111E-01	.13909E-02	.37538E-03	26	4	2	178
.00000E 00	.20550E 07	0	0	6	0	26	4	2	179

.35000E 00	.30300E 00	.14243E 00	.43333E-01	.17727E-02	.15769E-02	26	4	2	180
.00000E 00	.20990E 07	0	0	6	0	26	4	2	181
.33667E 00	.31800E 00	.14429E 00	.41444E-01	.33364E-02	.12308E-02	26	4	2	182
.00000E 00	.21510E 07	0	0	6	0	26	4	2	183
.41333E 00	.33600E 00	.15143E 00	.46889E-01	.60091E-02	.39308E-02	26	4	2	184
.00000E 00	.22000E 07	0	0	6	0	26	4	2	185
.41000E 00	.34000E 00	.15857E 00	.56444E-01	.10273E-01	.72077E-02	26	4	2	186
.00000E 00	.22430E 07	0	0	6	0	26	4	2	187
.38333E 00	.34000E 00	.16857E 00	.64333E-01	.11273E-01	.76923E-02	26	4	2	188
.00000E 00	.23000E 07	0	0	6	0	26	4	2	189
.36333E 00	.33600E 00	.17571E 00	.70111E-01	.11182E-01	.79231E-02	26	4	2	190
.00000E 00	.23500E 07	0	0	6	0	26	4	2	191
.36333E 00	.33600E 00	.17714E 00	.78444E-01	.13909E-01	.10231E-01	26	4	2	192
.00000E 00	.23980E 07	0	0	6	0	26	4	2	193
.36333E 00	.34000E 00	.18143E 00	.86222E-01	.15636E-01	.12077E-01	26	4	2	194
.00000E 00	.24480E 07	0	0	6	0	26	4	2	195
.38000E 00	.34400E 00	.18714E 00	.89333E-01	.16545E-01	.11923E-01	26	4	2	196
.00000E 00	.25000E 07	0	0	6	0	26	4	2	197
.42000E 00	.36000E 00	.19000E 00	.87222E-01	.16091E-01	.11077E-01	26	4	2	198
.00000E 00	.25500E 07	0	0	6	0	26	4	2	199
.43667E 00	.36800E 00	.19714E 00	.89667E-01	.17455E-01	.12769E-01	26	4	2	200
.00000E 00	.26000E 07	0	0	6	0	26	4	2	201
.44667E 00	.37000E 00	.20429E 00	.89000E-01	.16545E-01	.12231E-01	26	4	2	202
.00000E 00	.26500E 07	0	0	6	0	26	4	2	203
.46333E 00	.36600E 00	.20857E 00	.85333E-01	.14000E-01	.85385E-02	26	4	2	204
.00000E 00	.27000E 07	0	0	6	0	26	4	2	205
.47000E 00	.36400E 00	.21429E 00	.84889E-01	.12091E-01	.61077E-02	26	4	2	206
.00000E 00	.27500E 07	0	0	6	0	26	4	2	207
.45000E 00	.35600E 00	.21286E 00	.84889E-01	.10091E-01	.53923E-02	26	4	2	208
.00000E 00	.28000E 07	0	0	6	0	26	4	2	209
.46000E 00	.35800E 00	.21571E 00	.84556E-01	.89364E-02	.27308E-02	26	4	2	210
.00000E 00	.28500E 07	0	0	6	0	26	4	2	211
.46000E 00	.35800E 00	.21857E 00	.84222E-01	.67364E-02	.19538E-03	26	4	2	212
.00000E 00	.29000E 07	0	0	6	0	26	4	2	213
.46000E 00	.36400E 00	.22000E 00	.85222E-01	.71455E-02	.12692E-02	26	4	2	214
.00000E 00	.29500E 07	0	0	6	0	26	4	2	215
.45333E 00	.35600E 00	.21571E 00	.81111E-01	.53818E-02	.15538E-03	26	4	2	216
.00000E 00	.30000E 07	0	0	6	0	26	4	2	217
.46000E 00	.36000E 00	.22000E 00	.85000E-01	.70727E-02	.23077E-03	26	4	2	218
.00000E 00	.30500E 07	0	0	6	0	26	4	2	219
.46000E 00	.36000E 00	.22429E 00	.89000E-01	.86273E-02	.15769E-03	26	4	2	220
.00000E 00	.31000E 07	0	0	6	0	26	4	2	221
.47667E 00	.36800E 00	.23429E 00	.97667E-01	.12545E-01	.18692E-03	26	4	2	222
.00000E 00	.31500E 07	0	0	6	0	26	4	2	223
.49667E 00	.38000E 00	.24143E 00	.99222E-01	.13000E-01	.21385E-03	26	4	2	224
.00000E 00	.32000E 07	0	0	6	0	26	4	2	225
.52333E 00	.39600E 00	.24857E 00	.10167E 00	.13000E-01	.68538E-03	26	4	2	226
.00000E 00	.32500E 07	0	0	6	0	26	4	2	227
.53667E 00	.40200E 00	.25571E 00	.10467E 00	.15091E-01	.14385E-02	26	4	2	228
.00000E 00	.33000E 07	0	0	6	0	26	4	2	229
.55000E 00	.41200E 00	.25857E 00	.10489E 00	.14818E-01	.85385E-03	26	4	2	230
.00000E 00	.33500E 07	0	0	6	0	26	4	2	231
.55333E 00	.41000E 00	.25143E 00	.97556E-01	.12909E-01	.12462E-02	26	4	2	232
.00000E 00	.34000E 07	0	0	6	0	26	4	2	233
.55667E 00	.40600E 00	.25143E 00	.99444E-01	.12727E-01	.11308E-02	26	4	2	234
.00000E 00	.34500E 07	0	0	6	0	26	4	2	235
.56333E 00	.40600E 00	.25286E 00	.10156E 00	.16182E-01	.26077E-02	26	4	2	236
.00000E 00	.35000E 07	0	0	6	0	26	4	2	237
.56000E 00	.40200E 00	.25857E 00	.10889E 00	.18273E-01	.38769E-02	26	4	2	238
.00000E 00	.35500E 07	0	0	6	0	26	4	2	239

.55567E 00	.39800E 00	.25857E 00	.10911E 00	.19727E-01	.47077E-02	26	4	2	240
.00000E 00	.36000E 07	0	0	6	0	26	4	2	241
.56000E 00	.40000E 00	.26714E 00	.11889E 00	.22727E-01	.66077E-02	26	4	2	242
.00000E 00	.36500E 07	0	0	6	0	26	4	2	243
.55667E 00	.40000E 00	.27571E 00	.12222E 00	.24455E-01	.72462E-02	26	4	2	244
.00000E 00	.37000E 07	0	0	6	0	26	4	2	245
.55667E 00	.40800E 00	.27857E 00	.12667E 00	.23818E-01	.55769E-02	26	4	2	246
.00000E 00	.37500E 07	0	0	6	0	26	4	2	247
.56000E 00	.41000E 00	.28000E 00	.12778E 00	.24273E-01	.50308E-02	26	4	2	248
.00000E 00	.38000E 07	0	0	6	0	26	4	2	249
.56667E 00	.41400E 00	.28714E 00	.13333E 00	.25909E-01	.61385E-02	26	4	2	250
.00000E 00	.38500E 07	0	0	6	0	26	4	2	251
.57000E 00	.41600E 00	.28429E 00	.13000E 00	.22182E-01	.29154E-02	26	4	2	252
.00000E 00	.39050E 07	0	0	6	0	26	4	2	253
.57667E 00	.42400E 00	.28857E 00	.13556E 00	.26818E-01	.40000E-02	26	4	2	254
.00000E 00	.39550E 07	0	0	6	0	26	4	2	255
.58333E 00	.43200E 00	.29286E 00	.14222E 00	.31364E-01	.50000E-02	26	4	2	256
.00000E 00	.40000E 07	0	0	6	0	26	4	2	257
.58333E 00	.43200E 00	.29286E 00	.14222E 00	.31364E-01	.50000E-02	26	4	2	258
2.60000+	4 5.53650+	1	0	1	0	26	4	51	260
0.0	5.53650+	1	0	1	48	26	4	51	261
	48	2				26	4	51	262
.00000E 00	.10000E 07	0	0	2	0	26	4	51	263
.00000E 00	.00000E 00	.00000E 00	.00000E 00	.00000E 00	.00000E 00	26	4	51	264
.00000E 00	.15000E 07	0	0	2	0	26	4	51	265
.00000E 00	.00000E 00	.00000E 00	.00000E 00	.00000E 00	.00000E 00	26	4	51	266
.00000E 00	.17210E 07	0	0	4	0	26	4	51	267
-.14140E-01-	.45400E-02-	.11777E-02	.12122E-02	.00000E 00	.00000E 00	26	4	51	268
.00000E 00	.17610E 07	0	0	4	0	26	4	51	269
.49567E-02-	.92640E-02-	.20886E-02-	.21478E-02	.00000E 00	.00000E 00	26	4	51	270
.00000E 00	.18030E 07	0	0	4	0	26	4	51	271
.10550E-01-	.15966E-01-	.53900E-03-	.16167E-02	.00000E 00	.00000E 00	26	4	51	272
.00000E 00	.18470E 07	0	0	4	0	26	4	51	273
.13733E-01-	.21100E-01-	.54500E-03	.88267E-03	.00000E 00	.00000E 00	26	4	51	274
.00000E 00	.18940E 07	0	0	4	0	26	4	51	275
.16177E-01-	.23220E-01-	.46143E-03-	.45756E-03	.00000E 00	.00000E 00	26	4	51	276
.00000E 00	.19390E 07	0	0	4	0	26	4	51	277
.18040E-01-	.29160E-01-	.15514E-02-	.59622E-03	.00000E 00	.00000E 00	26	4	51	278
.00000E 00	.19880E 07	0	0	4	0	26	4	51	279
.15857E-01-	.34540E-01	.21543E-02-	.11967E-02	.00000E 00	.00000E 00	26	4	51	280
.00000E 00	.20410E 07	0	0	4	0	26	4	51	281
.14073E-01-	.30260E-01	.37329E-02-	.22033E-02	.00000E 00	.00000E 00	26	4	51	282
.00000E 00	.20960E 07	0	0	4	0	26	4	51	283
.12447E-01-	.29480E-01	.44743E-02-	.20433E-02	.00000E 00	.00000E 00	26	4	51	284
.00000E 00	.21470E 07	0	0	4	0	26	4	51	285
.13637E-01-	.27480E-01	.63514E-02-	.18400E-02	.00000E 00	.00000E 00	26	4	51	286
.00000E 00	.21980E 07	0	0	4	0	26	4	51	287
.17233E-01-	.24860E-01	.74800E-02-	.35211E-02	.00000E 00	.00000E 00	26	4	51	288
.00000E 00	.22400E 07	0	0	4	0	26	4	51	289
.13390E-01-	.21940E-01	.85914E-02-	.26244E-02	.00000E 00	.00000E 00	26	4	51	290
.00000E 00	.22830E 07	0	0	4	0	26	4	51	291
.18403E-01-	.17634E-01	.80586E-02-	.30633E-02	.00000E 00	.00000E 00	26	4	51	292
.00000E 00	.23270E 07	0	0	4	0	26	4	51	293
.20867E-01-	.14680E-01	.89929E-02-	.29478E-02	.00000E 00	.00000E 00	26	4	51	294
.00000E 00	.23700E 07	0	0	4	0	26	4	51	295
.26247E-01-	.19130E-01	.11004E-01-	.14089E-02	.00000E 00	.00000E 00	26	4	51	296
.00000E 00	.24110E 07	0	0	4	0	26	4	51	297
.27860E-01-	.17802E-01	.10989E-01-	.12967E-02	.00000E 00	.00000E 00	26	4	51	298
.00000E 00	.24540E 07	0	0	4	0	26	4	51	299

.30030E-01-.14214E-01	.99543E-02-.10648E-02	.00000E 00	.00000E 00	26	4	51	300
.00000E 00 .25000E 07	0	4	0	26	4	51	301
.23983E-01-.16002E-01	.10740E-01 .24522E-03	.00000E 00	.00000E 00	26	4	51	302
.00000E 00 .25500E 07	0	4	0	26	4	51	303
.25480E-01-.15310E-01	.92257E-02-.67244E-03	.00000E 00	.00000E 00	26	4	51	304
.00000E 00 .26000E 07	0	4	0	26	4	51	305
.20930E-01-.16254E-01	.75643E-02 .79678E-03	.00000E 00	.00000E 00	26	4	51	306
.00000E 00 .26500E 07	0	4	0	26	4	51	307
.18347E-01-.18494E-01	.48786E-02-.35244E-03	.00000E 00	.00000E 00	26	4	51	308
.00000E 00 .27000E 07	0	4	0	26	4	51	309
.11647E-01-.12670E-01	.31336E-02 .11667E-02	.00000E 00	.00000E 00	26	4	51	310
.00000E 00 .27500E 07	0	4	0	26	4	51	311
.14490E-01-.12196E-01	.16900E-02-.36400E-03	.00000E 00	.00000E 00	26	4	51	312
.00000E 00 .28000E 07	0	4	0	26	4	51	313
.13110E-01-.16254E-01	.24157E-02-.48400E-03	.00000E 00	.00000E 00	26	4	51	314
.00000E 00 .28500E 07	0	4	0	26	4	51	315
.18890E-01-.14216E-01	.21629E-02 .31622E-03	.00000E 00	.00000E 00	26	4	51	316
.00000E 00 .29000E 07	0	4	0	26	4	51	317
.21213E-01-.13178E-01	.35957E-02 .19878E-02	.00000E 00	.00000E 00	26	4	51	318
.00000E 00 .29500E 07	0	4	0	26	4	51	319
.22660E-01-.12472E-01	.53200E-02 .12233E-02	.00000E 00	.00000E 00	26	4	51	320
.00000E 00 .30000E 07	0	4	0	26	4	51	321
.24450E-01-.83520E-02	.71786E-02-.24133E-03	.00000E 00	.00000E 00	26	4	51	322
.00000E 00 .30500E 07	0	4	0	26	4	51	323
.31363E-01-.52440E-02	.66700E-02-.95300E-03	.00000E 00	.00000E 00	26	4	51	324
.00000E 00 .31000E 07	0	4	0	26	4	51	325
.32890E-01-.76420E-02	.74629E-02 .66733E-03	.00000E 00	.00000E 00	26	4	51	326
.00000E 00 .31500E 07	0	4	0	26	4	51	327
.37767E-01-.70060E-02	.49771E-02 .22367E-02	.00000E 00	.00000E 00	26	4	51	328
.00000E 00 .32000E 07	0	4	0	26	4	51	329
.36567E-01-.79820E-02	.45729E-02 .28822E-02	.00000E 00	.00000E 00	26	4	51	330
.00000E 00 .32500E 07	0	4	0	26	4	51	331
.34967E-01-.65960E-02	.42400E-02 .19900E-02	.00000E 00	.00000E 00	26	4	51	332
.00000E 00 .33000E 07	0	4	0	26	4	51	333
.33273E-01-.25520E-02	.69129E-02 .36011E-02	.00000E 00	.00000E 00	26	4	51	334
.00000E 00 .33500E 07	0	4	0	26	4	51	335
.25443E-01-.50260E-02	.84314E-02 .57600E-02	.00000E 00	.00000E 00	26	4	51	336
.00000E 00 .34000E 07	0	4	0	26	4	51	337
.20807E-01-.11296E-01	.11716E-01 .74200E-02	.00000E 00	.00000E 00	26	4	51	338
.00000E 00 .34500E 07	0	4	0	26	4	51	339
.17720E-01-.11158E-01	.13020E-01 .72389E-02	.00000E 00	.00000E 00	26	4	51	340
.00000E 00 .35000E 07	0	4	0	26	4	51	341
.14767E-01-.11320E-01	.17286E-01 .68156E-02	.00000E 00	.00000E 00	26	4	51	342
.00000E 00 .35500E 07	0	4	0	26	4	51	343
.12430E-01-.12916E-01	.18857E-01 .74411E-02	.00000E 00	.00000E 00	26	4	51	344
.00000E 00 .36000E 07	0	4	0	26	4	51	345
.10943E-01-.16220E-01	.21329E-01 .87111E-02	.00000E 00	.00000E 00	26	4	51	346
.00000E 00 .36500E 07	0	4	0	26	4	51	347
.16410E-01-.16176E-01	.22471E-01 .48289E-02	.00000E 00	.00000E 00	26	4	51	348
.00000E 00 .37000E 07	0	4	0	26	4	51	349
.31860E-01-.12674E-01	.21943E-01 .43678E-02	.00000E 00	.00000E 00	26	4	51	350
.00000E 00 .37500E 07	0	4	0	26	4	51	351
.42800E-01-.70620E-02	.22156E-01 .34400E-02	.00000E 00	.00000E 00	26	4	51	352
.00000E 00 .38000E 07	0	4	0	26	4	51	353
.48333E-01-.23320E-02	.23557E-01 .34176E-02	.00000E 00	.00000E 00	26	4	51	354
.00000E 00 .38500E 07	0	4	0	26	4	51	355
.48867E-01 .40780E-03	.23743E-01 .14333E-02	.00000E 00	.00000E 00	26	4	51	356
.00000E 00 .40000E 07	0	4	0	26	4	51	357
.48867E-01 .40780E-03	.23743E-01 .14333E-02	.00000E 00	.00000E 00	26	4	51	358
				26	4	0	359

2.60000+	4	5.53650+	1	0	0	0	0	26	4	52	360
0.0		5.53650+	1	1	2	0	0	26	4	52	361
2.60000+	4	5.53650+	1	0	0	0	0	26	4	0	362
0.0		5.53650+	1	1	2	0	0	26	4	53	363
2.60000+	4	5.53650+	1	0	0	0	0	26	4	53	364
0.0		5.53650+	1	1	2	0	0	26	4	0	365
2.60000+	4	5.53650+	1	0	0	0	0	26	4	54	366
0.0		5.53650+	1	1	2	0	0	26	4	54	367
2.60000+	4	5.53650+	1	0	0	0	0	26	4	0	368
0.0		5.53650+	1	1	2	0	0	26	4	55	369
2.60000+	4	5.53650+	1	0	0	0	0	26	4	55	370
0.0		5.53650+	1	1	2	0	0	26	4	0	371
2.60000+	4	5.53650+	1	0	0	0	0	26	4	56	372
0.0		5.53650+	1	1	2	0	0	26	4	56	373
2.60000+	4	5.53650+	1	0	0	0	0	26	4	0	374
0.0		5.53650+	1	1	2	0	0	26	4	57	375
								26	4	57	376
								26	4	0	377
								26	0	0	378
								-1	0	0	379

ACKNOWLEDGEMENTS

The authors are indebted to Dr. P. A. Moldauer for his helpful suggestions during this work and for the provision of the computational codes used in the model calculations.

REFERENCES

1. S. A. Cox and P. R. Hanley, IEEE Trans. Nucl. Sci., NS-18 No. 3, 108 (1971).
2. A. B. Smith, P. Guenther, R. Larson, C. Nelson, P. Walker and J. F. Whalen, Nucl. Instr. and Methods, 50 277 (1967); see also Phys. Ref., C12 1797 (1975).
3. P. T. Guenther, Elastic and Inelastic Neutron Scattering from the Even Isotopes of Tungsten, Thesis, Univ. of Illinois (1978).
4. A. Langsdorf, S. Monahan and W. Reardon, "Tabulation of Neutron Energies for Monoenergetic Protons on Lithium," Argonne National Laboratory Report, ANL-5219 (1954).
5. J. Hopkins and G. Breit, Nucl. Data, A9 137 (1971).
6. J. A. Harvey et al., Private Communication, data available from the National Nuclear Data Center, Brookhaven National Laboratory.
7. A. Smith and J. Whalen, "Comments on Energy-Averaged Neutron Total Cross Sections," Argonne National Laboratory Report, ANL/NDM-33 (1977).
8. E. Barnard, J. A. M. DeVilliers, C. A. Engelbrecht, D. Reitmann and A. B. Smith, Nucl. Phys., A118 321 (1968).
9. Evaluated Nuclear Data File-B, Version IV, National Nuclear Data Center, Brookhaven National Laboratory.
10. B. Holmqvist, and T. Wiedling, Proc. Int'l. Conf. on Nuclear Data for Reactors, Helsinki, Vol.-2, 327, IAEA Press Vienna (1970); symbol Δ for elastic and inelastic scattering.
11. Y. Tomita, K. Tsukada, M. Maruyama, S. Tanaka, Proc. Int'l. Conf. on Nuclear Data for Reactors, Helsinki, Vol.-2, 301, IAEA Press Vienna (1970); symbol +.
12. K. Tsukada, S. Tanaka, Y. Tomita and M. Maruyama, Nucl. Phys., A125 641 (1969); symbol x.
13. W. Gilboy and J. Towle, European-American Nuclear Data Committee Report, EANDC(UK)-465. Data available from the National Nuclear Data Center, Brookhaven National Laboratory; symbol \diamond .
14. H. Landon, A. Elwyn, G. Glasoe and S. Oleska, Phys. Rev., 112 1192 (1958).
15. L. Cranberg and J. Levin, Phys. Rev., 103 343 (1952); symbol \leftarrow .

16. J. Beyster and M. Walt, Phys. Rev., B104 19 (1956); symbol \boxtimes .
17. V. Popov et al., Jour. Nucl. Energy, 9 9 (1959).
18. R. Becker, W. Guindon and G. Smith, Nucl, Phys., 89 154 (1966).
19. M. Mackwe, D. Kent and S. Snowdon, Phys. Rev., 114 1563 (1959).
20. C. Muelhause, S. Bloom, H. Wegner and G. Glasoe, Phys. Rev., 103 720 (1956).
21. F. G. Perey, G. T. Chapman, W. E. Kinney and C. M. Perey, Proc. of Specialists Meeting on Neutron Data of Structural Materials for Fast Reactors, Pergamon Press, Oxford (1977).
22. M. N. Rao, Nuclear Data Sheets for A=56, B3-3, 4-43 (1969).
23. See Ref. 15; symbol +.
24. J. Hopkins and M. Silbert, Nucl. Sci. and Eng., 19 431 (1964); symbol = z.
25. J. Lindlow, Thesis, Case-Western Reserve Univ. (1970); Data available from the National Nuclear Data Center, Brookhaven National Laboratory; symbol \boxtimes .
26. See Ref. 12; inelastic-scattering symbol \uparrow .
27. See Ref. 13; symbol \boxtimes .
28. A. B. Tucker, J. T. Wells and W. E. Meyerhof, Phys. B137 1181 (1965); symbol *.
29. W. E. Kinney and F. G. Perey, Neutron Elastic and Inelastic Scattering Cross Section for ^{56}Fe in the Energy Range 4.19 to 8.56 MeV, Oak Ridge National Laboratory Report, ORNL-4515 (1970); symbol \diamond .
30. See Ref. 25; symbol \boxtimes .
31. W. E. Kinney and F. G. Perey, ^{54}Fe Neutron Elastic and Inelastic Scattering Cross Sections from 5.5 to 8.5 MeV, Oak Ridge National Laboratory Report, ORNL-4907; also W. E. Kinney and F. G. Perey, Neutron Elastic and Inelastic Scattering Cross Section for ^{56}Fe in the Energy Range 4.19 to 8.56 MeV, Oak Ridge National Laboratory Report, ORNL-4515 (1970); symbol \diamond .
32. B. Jennings, J. Weddell, I. Alexeff and R. Hellens, Phys. Rev., 98 582 (1955).
33. D. L. Smith, "Fast-Neutron Gamma-Ray Production from Elemental-Iron: $E_n \sim 2$ MeV," Argonne National Laboratory Report, ANL/NDM-20 (1976).

34. W. Hauser and H. Feshbach, Phys. Rev., 87 366 (1952).
35. P. Hodgson, "The Optical Model of Elastic Scattering" Oxford Press, London (1963).
36. H. Hofmann, J. Richert, J. Tepel and H. Weidenmüller, Ann. Phys. (NY), 90 403 (1975).
37. A. Gilbert and A. G. W. Cameron, Can. Jour. Phys., 43 1446 (1965).
38. B. Holmqvist and T. Wiedling, Aktiebolaget Atomenergi Report, AE-430 (1971).
39. P. H. Stelson and L. Grodzins, Nucl. Data, A1 21 (1965).
40. A. Smith, P. Guenther, D. Smith and J. Whalen, "The Interaction of Fast Neutrons with ^{60}Ni ," Argonne National Laboratory Report, ANL/NDM-44 (1979).
41. R. McKnight, Private Communication (1979).